Research Square

Preprints are preliminary reports that have not undergone peer review.
They should not be considered conclusive, used to inform clinical practice,
or referenced by the media as validated information.

Rethinking the Immune Responses Induced by Commercial Multicomponent Acellular and Whole Cell Pertussis Vaccines and Pertussis Infection in the Baboon Model

Yihui Wang
yihui.wang@fda.hhs.gov
United States Food and Drug Administration
Jonatan Maldonado Villeda
United States Food and Drug Administration
Tod Merkel
United States Food and Drug Administration

Article

Keywords: Pertussis, multicomponent vaccines, infection, baboon

Posted Date: November 5th, 2026

DOI: https://doi.org/10.21203/rs.3.rs-11568528/v1

License: This work is licensed under a Creative Commons Attribution 4.0 International License. Read Full License

Additional Declarations: No competing interests reported.

Abstract

Following the replacement of whole cell pertussis (wP) vaccines with acellular pertussis (aP) vaccines, high-income countries recorded sustained increases in pertussis cases. While aP vaccines protect against severe disease, they fail to prevent colonization and transmission, unlike wP vaccination and natural infection. The mechanisms underlying these differences remain incompletely understood. Trivalent aP vaccines are often characterized as inducing Th2 biased responses due to alum adjuvant. However, most current formulations of aP are combination vaccines containing additional antigens, which may shape the overall immune environment and influence responses to pertussis antigens.

To investigate these differences, we profiled immune responses in baboons following aP vaccinations, wP vaccinations and infections using complete blood counts, transcriptomics, and immunological assays. Weighted gene co-expression network analysis revealed fundamental differences in immune polarization. These findings define divergent immune landscapes induced by these three exposures, providing mechanistic insight into their differential protective efficacy and highlighting the importance of vaccine composition in shaping immune responses. Notably, our data suggest that pentavalent aP vaccination may induce distinct innate and cellular immune responses compared to trivalent formulations, with important implications for future vaccine design strategies, and design of clinical trials.

INTRODUCTION

Whooping cough is a highly contagious acute respiratory illness caused by the Gram-negative bacterial pathogen *Bordetella pertussis*. While usually mild in older children and adults causing runny nose, low-grade fever, and mild cough, pertussis can be severe in infants with symptoms including severe bouts of coughing, apnea, pneumonia, and death[1]. Despite high rates of vaccination, pertussis remains a major cause of vaccine-preventable morbidity and mortality.

Pertussis is transmitted through respiratory droplets from infected individuals, including those who are asymptomatic[2]. Symptoms typically appear within 5 to 10 days of exposure and begin as a mild upper respiratory infection before progressing to severe paroxysmal coughing episodes, often accompanied by the characteristic high-pitched "whoop" sound upon inhalation and frequently resulting in post-tussive vomiting and cyanosis, leaving patients severely exhausted. These episodes can persist for up to 10 weeks. In infants, pertussis can result in permanent disability and even death. While not lifelong, this natural immunity confers near-complete protection upon subsequent exposure to pertussis[3] and has long been regarded as the gold standard for protection against reexposure.

The first use of whole cell pertussis (wP) vaccines in the U.S. was documented in 1914[4]. They were relatively crude and were not routinely used for widespread childhood immunization. In the 1940s, improved wP vaccines were developed and were combined with diphtheria and tetanus toxoids to form the whole-cell DTP vaccine. Wide-spread use of DTP vaccines brought the number of annual pertussis cases from 115,000–270,000 down to 1,200–4,000, and the number of annual deaths caused by pertussis down from 5,000–10,000 to five - ten[5]. However, the reactogenicity of wP vaccines resulted in reduced public acceptance over time stimulating the development and introduction of less-reactogenic acellular pertussis (aP) vaccines in the form of DTaP in the 1990s. These DTaP vaccines demonstrated comparable efficacy to the DTP vaccines they replaced in clinical trials[6–10]. In the years following introduction of DTaP, multicomponent DTaP-containing vaccines (DTaP-IPV, DTaP-Hib-IPV, and DTaP-Hib-HepB-IPV) were licensed in the US with the additions of inactivated poliovirus, *Hemophilus influenzae* type b polyribosylribitol phosphate (PRP) conjugated to carrier proteins, and hepatitis B surface antigen. Recent market research show 96% of aP vaccines distributed in the U.S. are pentavalent or hexavalent[11,12]. The aP vaccines currently used in the U.S. contain chemically detoxified pertussis toxin (PT), filamentous haemagglutinin (FHA), and pertactin (PRN). Some also include fimbriae (FIM). In the past decade, CDC surveillance has shown consistently high national vaccination coverage with over 92% of children receiving three aP doses by 24 months of age, and more than 87% receiving four aP doses by 35 months of age[13]. Despite these high vaccination rates, the implementation of aP coincides with a steady increase in the number of reported pertussis cases[14]. Notably, over 48,000 cases and over 43,000 cases were reported in the U.S. in 2012 and 2024, respectively[14,15]. Accumulating evidence from animal models and epidemiological surveillance indicates that currently licensed aP vaccines protect against disease but provide incomplete protection against infection, carriage or transmission, underscoring the need for next generation pertussis vaccines with improved societal benefit[16,17]. Despite renewed interest and significant effort towards development of improved vaccines, the immune correlates of protection against *B. pertussis* colonization remain unknown but are likely to involve both humoral[18,19] and cellular immune[20,21] responses.

Both pertussis infection and vaccination with the wP vaccine induce T helper type 1 (Th1) and type 17 (Th17) dominated responses, along with antibody responses targeting a broad array of bacterial antigens. These responses have been shown to prevent or reduce colonization and prevent symptomatic disease[3,22,23]. In contrast, the aP vaccines in the presence of alum adjuvant have been shown to induce T helper type 2 (Th2) dominated responses, eliciting antibodies directed against a limited set of antigens, along with an excellent safety profile. These responses prevent symptomatic disease but fail to prevent colonization, carriage and transmission[3,17]. Recent studies using mouse models of airway infection with *B. pertussis* and analyses of human samples have demonstrated that bacterial clearance from the airway requires IL-17 and IFN-γ secreting tissue resident memory T cells, which are induced by natural infection and wP vaccination but not by aP vaccination[24]. However, it's worth noting that most if not all of these studies used the commercial trivalent DTaP vaccines, Daptacel or Infanrix, or used research grade aP vaccines composed of individual pertussis antigens and adjuvanted with alum[3,17,22,25,26]. Considering the widespread use of pentavalent and hexavalent aP vaccines and known ability of viral antigens to function as potent innate immune activators, we examined the immune responses induced by these vaccines in comparison with the responses induced by wP vaccines and natural infection.

To dissect differences in immune responses to vaccination with pentavalent commercial aP vaccine (DTaP-Hib-IPV), commercial pentavalent wP vaccine (DTwP-Hib-HepB + IPV), and infection that may explain differences in the protection conferred by each type of exposure, we used the baboon model and performed extensive sample collection before and following each type of exposure. We used a systems biology approach to quantify changes in cellular composition, gene expression, antibody responses, and cytokine production during the early post-immunization period. We subsequently characterized the

pertussis specific humoral and cellular immune responses following completion of the primary vaccination series. Our analyses revealed distinct immune trajectories across immunization strategies and revealed differences in innate and adaptive immune signaling, which provides a foundation for understanding the duration of immunity of these immunization strategies and identifying potential correlates of protection against pertussis.

RESULTS

Baboon model of pertussis vaccination and infection for comparative immune profiling.

To compare the immediate immune responses following vaccination or infection, we vaccinated 12 baboons with commercial multivalent aP vaccine (Pentacel, Sanofi) and 12 baboons with commercial multivalent wP vaccine (Pentavac, Serum Institute of India) and IPOL (Sanofi), at 2, 4, and 6 months of age. IPOL was added to the wP vaccine group to match the polio component included in Pentacel. To enable comparisons of vaccine-mediated immune responses to responses induced by infection, we challenged 12 unvaccinated baboons with *B. pertussis* strain D420 at around 10 months of age (Figure 1A). During the vaccination phase, blood samples were collected before and after each dose to characterize the vaccine induced immune responses including complete blood cell counts (CBC), antibody titers against pertussis, serum cytokine responses, and transcriptomics of peripheral blood cells. On day 17 post the last dose of vaccination, PBMCs were isolated from blood for evaluating the immediate vaccine induced pertussis-specific cellular responses following restimulation with *B. pertussis* (Figure 1A). The same samples were collected from the challenged baboons just prior to and at matched time points after the inoculation (Figure 1A).

aP, wP vaccinations and infection elicit distinct cellular and transcriptional signatures in the peripheral blood illustrated by CBC and gene expression analysis.

Pertussis infection in naive animals is known to induce leukocytosis, particularly lymphocytosis, which was captured by CBC measurements. We observed peak monocyte counts at day 3, neutrophil counts at day 7, and lymphocyte and total white blood cell (WBC) counts at day 10 post challenge (Figure 1B and Table S1). Significant increases in lymphocyte and total WBC counts were observed following first dose of wP but not following the first dose of aP. Following the second dose of both vaccines, an influx of lymphocytes was observed in peripheral blood at day 8, reflecting immune activation in response to the repeated stimuli. In addition, eosinophil counts were significantly increased following both aP and wP vaccination as well as pertussis infection. Basophil elevation was more pronounced in the wP group, although modest increases were also observed after the second dose in both vaccination groups and during infection. The expansion of these granulocytes was accompanied by the significant induction of serum GM-CSF on days 3 and 8 following vaccination, and day 8 following infection (Figure 1C). A significant reduction in red blood cell (RBC) counts was observed across all groups, which may reflect early sampling associated blood loss or inflammation-driven hematological changes (Figure 1B and Table S1).

To characterize transcriptional responses, peripheral blood samples collected before and on days 1, 3, and 8 following the first vaccination for the vaccinated groups, and on days 3, 7, and 14 following pertussis challenge for the challenged group. These samples were subject to mRNA sequencing. A substantially higher number of upregulated differentially expressed genes (DGEs) were observed on day 8 following aP vaccination relative to earlier time points, coinciding with the enrichment of pathways related to the immunoglobulin complex and erythrocyte differentiation (Figure 1D and 1E). In contrast, a substantially higher number of genes in the wP group were downregulated on day 8 relative to earlier time points. A pattern of downregulation was even more prominent in the infection group, suggesting more complex immune modulation following these exposures (Figure 1D). Principal component analysis (PCA) revealed distinct temporal separation among the groups, with the wP vaccine and infection groups showing larger transcriptional changes over time compared to the aP vaccine group. (Figure 1F).

Gene set enrichment analysis (GSEA) was performed using ranked gene lists derived from differential expression relative to baseline. Curated gene sets were obtained from the Gene Ontology (GO) term collections using Ensembl biomaRt[27]. Enrichment scores (ES) were calculated by a weighted Kolmogorov–Smirnov–like running-sum statistic, and normalized enrichment scores (NES) were computed to account for differences in gene set sizes[28]. In aP vaccinated animals, antiviral innate immune responses dominated at day 1, followed by expansion of humoral immune pathways at day 8 (Figure 1E and Figure 2A). Although enrichment of immunoglobulin related pathways was also observed at day 8 in wP vaccinated animals, early responses were dominated by pathways related to vesicle secretion, RNA processing, apoptosis, and translation. A similar pattern was observed in the infected group, with even stronger enrichment of translation associated pathways and comparatively weaker humoral immune signatures (Figure 1E).

WGCNA identifies co-expressed gene modules corresponding to biological pathways and immune cell populations.

To characterize coordinated transcriptional changes in peripheral blood over time that may not be fully resolved by contrast-based GSEA, we performed unsupervised weighted gene co-expression network analysis (WGCNA) and identified 13 modules of highly co-expressed genes[29,30]. Each module was summarized by its module eigengene (ME) representing the first principal component of the module and capturing the overall temporal expression pattern within each group (Table 2). Because eigengenes are derived from correlation-defined modules, their absolute scale and baseline offset are dataset-dependent; thus, interpretation centers on relative longitudinal changes within each group rather than cross-group magnitude comparisons (Figure 1G). Functional enrichment analysis of genes in each module identified significantly associated biological programs (Table S2 and S3 csv file). These annotations suggest the coordinated functional pathways and/or putative cell populations represented in each module[30,31].

aP vaccination induces robust antiviral and cytotoxic responses not observed following wP vaccination or pertussis infection.

Multiple gene sets related to antiviral responses and innate immune responses were significantly enriched in the peripheral transcriptome isolated from animals on day 1 post aP vaccination (Figure 2A). Within these gene sets, many genes encoding interferon-stimulated antiviral effectors, including *OAS1*, *RSAD2*, *EIF2AK2*, and *MX1*, were significantly upregulated relative to baseline. Consistent with the GSEA results, WGCNA identified ME9 as a module enriched for genes involved in antiviral innate immunity, type I interferon (IFN) signaling, and viral sensing related pathways (Table 2, Table S2 and S3). ME9 showed significant upregulation on day one in aP vaccinated animals, whereas no comparable induction was observed in the wP or infection groups (Figure 1E).

To further characterize the magnitude and signaling cascades underlying the antiviral response including interferon responses, Th1 polarization, and the expression of cytotoxic effectors, we curated representative genes involved in these functional categories and visualized their expression patterns across time points within each group (Figure 2B). Differential expression significance compared to their respective baselines was calculated accordingly (Figure 2B and Table S4). Baboon Ensembl gene identifiers were mapped to human orthologous gene symbols with Ensembl database to facilitate biological interpretation (see Method). In aP vaccinated animals, we observed significant upregulation of genes encoding viral nucleic acid pathogen-recognition receptors (PRRs), including *TLR3*, *TLR7*, *RIGI* and *IFI16*, along with associated regulators (*DHX58*, *DDX60*)[32,33]. The expression of these PRRs is induced not only by viral nucleic acid sensing but also via type I IFN feedback amplification[34]. Although the gene expression of relevant IFN regulatory factors (IRFs) and signal transducers and activators of transcription (STAT) showed modest elevation at day 1 in aP vaccinated animals, these changes did not reach statistical significance. No significant difference was detected in the expression of IFN receptors or IFN cytokines across groups. Nevertheless, type I IFN-stimulated genes (ISGs) encoding antiviral effectors were robustly and significantly upregulated in the same animals (Figure 2B). Given that the antiviral responses frequently promote Th1 differentiation, we examined the related markers. Expression of *IL27* encoding IL-27p28 and the Th1 master transcription factor *TBX21* (T-bet) were elevated at day 1 post aP vaccination, with *TBX21* reaching significant upregulation by day 8. However, these transcriptional signatures were not accompanied by increased serum IFN-γ production (data not shown), suggesting tightly regulated or localized Th1 responses. Transcriptional changes in Th1 polarization presented differently in the wP and infection groups. We observed significant elevation in the expression of *STAT4* in wP vaccinated animals, which has been shown to enhance Th1 differentiation and the induction of cellular immunity (Figure 2B)[35]. A mild elevation in serum IL-27p28 production was observed on day 3 post aP or wP vaccination followed by a significant increase in IL-27p28 production in serum observed on day 8 in the infected animals (Figure 2C). IL-27 promotes expansion of Th1 cells by activating STAT1-mediated T-bet signaling pathway[36]. However, accumulating evidence indicates that IL-27 also participates in diverse regulatory mechanisms that prevent immune hyperactivity[37]. The robust but delayed increase in serum IL-27p28 observed in infected animals may reflect the complex role of IL-27 in supporting antimicrobial immunity while subsequently constraining excessive inflammation.

Following the early antiviral responses, WGCNA module ME10, which is enriched for genes associated with cytotoxic immune responses, was significantly upregulated at day 3 in aP vaccinated animals (Table 2 and Figure 1G). This module included cytotoxic effector genes *NKG7*, *PRF1*, and *GZMB*, suggesting activation of natural killer (NK) cells and cytotoxic T cells (Figure 2D)[38]. This cytotoxic response was further illustrated by the upregulation of *IL15RA* and *IL2RB* which are involved in promoting NK cell differentiation and survival, as well as *FCGR3A* (CD16), which mediates antibody-dependent cellular cytotoxicity, and *CCL5*, which is involved in immune cell recruitment (Figure 2D)[39]. In contrast, in the wP-vaccinated and infected animals, the expression of *CD27*, *CD8A*, and *CD8B* were significantly elevated suggesting antigen-driven expansion of adaptive cytotoxic T cells following these exposures (Figure 2D).

Pertussis infection and wP vaccination induce strong inflammatory responses through NFkb-Th17-neutrophil axis.

Given the strong induction of viral nucleic acid sensing PRRs in aP vaccinated animals, we next examined the expression of other PRR families across the three exposure groups. All groups showed modest early elevation of Toll-like receptor (TLR) transcripts, although these changes did not reach statistical significance (Figure 3A). Pertussis infection induced strong expression of C-type lectin receptors (CLRs), particularly *CLEC4D* (Figure 3A). CLRs recognize a diverse range of ligands including polysaccharide, glycoproteins, and glycolipids from fungi, mycobacteria, and certain viruses, as well as endogenous damage-associated molecular patterns (DAMPs) released during tissue injury or necrotic cell death[40]. The expression of CLRs can be induced not only by direct innate sensing of these PAMPs and DAMPs but also by inflammatory cytokines such as TNF-α, IL-1β, and IFN-γ[41]. CLR signaling is a potent driver of Th17 immune responses through activation of NF-κB[40,41]. We next examined the expression of these signals and observed significant elevation and stronger expression of *NFKB1* and *NFKB2* in both the infection and wP vaccination groups (Figure 3B). This activation was followed by upregulation of the transcription factor *RORA* in the infection group, which is required for Th17 differentiation and IL-17 production[42], as well as increased expression of IL-6 and IL-23 signaling, with corresponding cytokines productions detected in serum (Figure 3B-D). As a central pro-inflammatory mediator, IL-6 plays a critical role in acute phase responses and, together with TGF-β, promotes the differentiation of naïve CD4 T cells into Th17 cells[43,44]. IL-23 is required for the maintenance and expansion of Th17 populations[45]. Consistent with this amplification loop, we found that *CCR6*, encoding a chemokine receptor associated with Th17 cell recruitment and mucosal homing[45], was significantly upregulated in the infection group. Both the infection and the wP groups also exhibited elevated expression of *CCR7*, a marker associated with lymphoid tissue trafficking, and *CXCR4*, suggesting enhanced immune cell chemotaxis and lymphoid tissue migration[46].

Th17 immune responses are known to drive neutrophilic inflammation by inducing inflammation in local stromal and epithelial cells that promote neutrophil recruitment from peripheral blood[47]. In line with elevated Th17 signatures and chemotactic signals, we observed a strong neutrophil influx in animals during pertussis infection (Figure 1B and 3E). Furthermore, module ME2 identified by WGCNA showed a significant correlation with neutrophil counts across all

groups (Figture 3F and Table 2). Within this module, genes encoding inflammatory alarmins *S100A8*, *S100A9*, and *S100A12* were significantly upregulated in the infected animals. These molecules also function as DAMPs[48], amplifying inflammatory responses (Figure 3B). *CD177*, a marker expressed by activated neutrophils[49], was significantly elevated during pertussis infection, but only transiently upregulated at day 1 following wP vaccination.

Although most neutrophil granule proteins are synthesized during granulopoiesis in the bone marrow, active transcription of many granule genes can be detected in peripheral blood during inflammation, which likely reflects the mobilization of immature granulocytes released during emergency granulopoiesis[50]. Importantly, increased expression of these granule-associated genes does not necessarily indicate neutrophil degranulation. Rather, it most likely reflects a shift in the circulating neutrophil compartment toward immature neutrophil populations, resulting in increased abundance of granule-associated transcripts (Figure 3G).

aP vaccination induces alum associated type 2 signatures, whereas wP and infection exhibit Th2 polarization.

To characterize the role of aluminum phosphate adjuvant in Pentacel (aP) and Pentavac (wP), we examined the expression of genes associated with inflammasome activation, type 2 immunity, and their downstream effector pathways. We observed increased expression of *NLRP3*, *PYCARD*, and *CTSB* at day 1 following aP vaccination, with *NLRP3* and *CTSB* reaching statistical significance (Figure 4A). Upregulation of these genes suggests activation of the NLRP3 inflammasome pathway, likely reflecting cellular stress following particulate stimulation[51,52]. In addition, we observed elevated expression and production of the alarmin *IL33* and its receptor *IL1RL1* (ST2) at day 3 and 8 following aP vaccination, suggesting engagement of IL-33 mediated signaling pathways known to promote type 2 immunity (Figure 4A)[53]. Although strong inductions of the canonical Th2 associated markers *IL4R* and *GATA3* were not observed, increased expression of *IRF4*, a transcription factor critical for Th2 differentiation, and humoral immune responses was detected on day 8 (Figure 4A). In parallel, enrichment of *IL5RA* and *CCR3* is consistent with an increased abundance and/or activation of eosinophils[54], while *ALOX15* expression reflects lipid mediator production associated with type 2 inflammation and tissue remodeling (Figure 4A)[55]. Finally, elevations of *IGHE* expression and total IgE production in serum was observed following the first dose of aP and wP vaccination or infection, likely reflecting generalized immune activation associated with inflammatory responses, although pertussis toxin activity has been implicated in generation of IgE in mice[56,57]. Following the second and third vaccination doses, total serum IgE returned to baseline in animals vaccinated with wP. In contrast, the elevation of serum total IgE persists after the second and third aP vaccinations, which may suggest a sustained type 2 immunity-driven humoral responses rather than a transient consequence of generalized immune activation (Figure 4A and 4B).

Although the inflammasome-alarmin-eosinophil transcriptional signature was absent, both the wP and infection groups exhibited evidence of Th2 development, indicated by significant upregulation of *GATA3*, a master regulator of Th2 immunity but also involved in T cell development[58], and *IL4R*, which plays critical roles in IL-4 and IL-13 signaling (Figure 4A). This pattern may reflect antigen-driven adaptive Th2 differentiation rather than alum triggered innate type 2 responses initiated through tissue damage and alarmin release. Accompanying the observation of transcriptional changes, CBC analysis revealed increased circulating eosinophil counts in the peripheral blood across all groups, and increased basophil counts in both vaccinations although was only significant in the wP group (Figure 1A, 4C and 4D). Noticeably, significant inductions of eosinophil and basophil counts were observed post the second dose of vaccination in both groups with no significant difference between them (Figure 1A, 4E and 4F). However, these hematological changes likely reflect a combination of generalized inflammatory responses, enhanced granulopoiesis, and altered leukocyte trafficking, and therefore should not be interpreted as direct evidence of type 2 immune polarization in isolation.

Immunization induces transient red blood cell reduction with aP specific association to erythropoietic responses.

Following the first dose of aP and wP vaccination, we observed a significant reduction in RBC counts (Figure 1A). Although this decrease could partially reflect blood volume loss due to repeated sampling in young animals, a similar reduction was observed after the second vaccination dose in both groups, despite minimal blood collection limited to day 0 (vaccination day) and day 8 (Figure 1A and 1B). Over the course of the vaccination series, aP vaccinated animals exhibited slightly greater reduction in RBC compared to the wP group (Figure 5A and 5B). Accompanying this observation, transcriptional signatures associated with erythrocyte differentiation and heme biosynthesis were significantly upregulated in aP vaccinated animals as identified by both GSEA and WGCNA (ME4) analyses (Figure 1E and 1G, Table 2). Notably, WGCNA module ME4 enriched for erythropoiesis related genes showed a significant correlation with RBC reduction specifically in the aP group but not in the wP or the infection groups (Figure 5C). A comparable decrease in RBCs was also observed during pertussis infection (Figure 1B and unpublished data) suggesting a broader response to immunological stimuli, potentially driven by shifts in hematopoietic output favoring leukocyte expansion.

aP vaccination induces coordinated complement, coagulation, and platelet associated transcriptional signatures.

WGCNA revealed that aP vaccinated animals exhibited upregulation of module ME8 at days 1 and 3 post immunization, which is enriched for genes associated with complement pathways (Figure 1G and Table 2). Closer examination showed increased transcription of multiple complement related genes involved in both activation and regulatory processes, including significant upregulation of *C5*, *C3AR1*, *C5AR2*, and *CLU* (Figure 5D). *C3AR1* and *C4BPB* were significantly upregulated in the wP and infection groups. While *C3AR1* encodes the receptor for C3a and mediates inflammatory responses in myeloid cells[59],

C4BPB encodes a soluble regulator of the classical and lectin complement pathways that limit excessive complement activation and protects host tissue[60]. Additionally, the complement regulator *CLU* was also significantly upregulated in infected animals (Figure 5D). Although transcriptional changes in complement components and regulators do not necessarily indicate active complement cascade engagement, they may imply a primed and tightly regulated complement system.

The complement system is closely interconnected with coagulation and platelet activation within the broader network of immunothrombosis[61,62]. Consistent with this, we observed significant upregulation of module ME5 at day 3 post aP vaccination, which is enriched for genes involved in coagulation and platelet regulations (Figure 1G and Table 2). Among the related genes, *SERPINE1*, *F13A1*, and *THBD* were significantly upregulated, indicating active regulation of coagulation and fibrinolytic balance. Meanwhile, increased expression of *F2RL3* (PAR4), *ITGA2B* (CD41), *SELP* (P-selectin), and *PPBP* (CXCL7) suggest platelet activation and platelet-mediated inflammatory responses, including leukocyte recruitment and tissue remodeling (Figure 5D). Platelet counts were significantly increased across all groups following initial exposure (Figure 1B), despite the more pronounced transcriptional signatures of complement, coagulation, and platelet pathways in the aP group. Finally, the increased expression of *IL33* and its receptor *IL1RL1* may indicate heightened tissue stress in the aP group (Figure 4A), which could contribute to the preferential engagement of these pathways.

Distinct innate and cell mediated regulatory responses across immunization groups.

We next examined the expression of regulatory and immune checkpoint associated genes across groups. Following immunizations, all groups showed significant upregulation of *TGFBI*, which encodes a TGF-β inducible extracellular matrix protein (βig-h3) involved in tissue remodeling and may be associated with immune regulatory processes (Figure 5E)[63,64]. Both the wP and the infection groups showed significant upregulation of *IL4I1*, an immunoregulatory enzyme linked to myeliod cell mediated immune suppression[65,66]. In contrast, only the infection group showed significantly increased expression of *IL37*, a potent anti-inflammatory cytokine of the IL-1 family (Figure 5E)[67], indicating a strong counter-regulatory response to inflammation. In contrast to these innate regulatory signals observed in the wP and infection groups, we observed significant upregulation of *FOXP3*, a canonical marker of regulatory T cells, as well as *NR4A1* and *TOX2*, transcription factors associated with T cell anergy and exhaustion in the aP group (Figure 5E)[68]. Although not reaching statistical significance, aP vaccinated animals also showed elevated expression of inhibitory checkpoint related gene, including *CTLA4*, *LAG3*, and *HAVCR2* (Figure 5E)[69]. Collectively, these observations suggests that distinct regulatory pathways are engaged across immunization groups, with wP and infection groups showing stronger innate immunoregulatory signatures while aP vaccination associated with signatures of T cell regulation and checkpoint activation.

Differential plasma cell, germinal center, and memory B cell signatures define distinct humoral immune responses across immunization groups

Pathway analysis by both GSEA and WGCNA (ME11) revealed differential expressions of genes associated with the immunoglobulin complex and antibody mediated immunity (Figure 1E, 1G and Table 2). Closer examination showed that multiple genes encoding immunoglobulin heavy chain variable regions (*IGHV*), together with *IGKC*, *IGHM*, and *IGHE*, belonging to module ME11, were significantly upregulated at day 8 following both aP and wP vaccination, but not during pertussis infection (Figure 6A, 4A and Table S2). In parallel, we observed significant upregulation of *IRF4, XBP1* and *MZB1* at day 8 in aP vaccinated animals, whereas only *MZB1* was significantly increased in the wP group (Figure 4A and 6A). Both *IRF4 and XBP1* are enriched in plasma cells[70], and *MZB1* play important roles in supporting immunoglobulin folding and secretion[71]. Consistent with this, signals related to plasma cell survival were also increased, including significant upregulation of *TNFSF13* (APRIL) in the aP group and *TNFRSF17* (BCMA) in both aP and wP groups[70]. Together, these signatures suggest active plasma cell differentiation, survival, and antibody secretion in both vaccination groups.

Since durable and high affinity humoral immunity depends on germinal center (GC) activation and T follicular helper (Tfh) cell engagement, we next examined genes involved in GC formation, memory B cell maintenance, and Tfh commitment. The infection group showed significant upregulation of *CXCR5*, a chemokine receptor required for follicular and germinal center trafficking[72]; *TNFRSF13C* (BAFFR), which promotes B cell survival[73]; *FCRL2*, a marker enriched in memory B cells[74]; and the transcriptional repressors *BACH2* and *PAX5*, which inhibit plasma cell differentiation and maintain memory B cells lineage[70]. Collectively, these signatures from the infection group suggest a bias toward germinal center activity and memory B cell maintenance, with relative restraint of terminal plasma cell differentiation. Mirroring these responses, the wP group also showed significantly upregulated of *FCRL2*, *BACH2* (Figure 6A). In addition, although not statistically significant, both the infection and wP groups showed elevated expression of *BCL6*, the transcription factor required for both germinal center B cells and Tfh cells[75,76]. In contrast to the stronger plasma cell bias observed in the aP group and the memory/GC skewed signatures seen during infection, wP vaccinated animals appeared to exhibit a more balanced plasma cell differentiation and memory B cell commitment.

Finally, we examined the expression of Fc receptors, which are critical mediators for antibody effector functions. Following immunizations, all groups showed increased expression of multiple Fc receptors. Both the aP and infection groups significantly upregulated *FCGR1A* (CD64), a high-affinity IgG receptor that mediates phagocytosis and cytokine production in monocytes, macrophages and neutrophils[77]. The aP vaccination also strongly increased the expression of *FCGR3A* (CD16), which was discussed previously (Figure 2D). Lastly, we observed marked elevation in the expression of IgA receptor (*FCAR*), IgA heavy chain (*IGHA1*), and the significant upregulation of *JCHAIN* in the infection group, suggesting enhanced IgA mediated effector function consistent with more mucosal oriented immune responses (Figure 6A).

Accompanying the transcriptional changes, we evaluated the serum IgG responses against *B. pertussis* whole cell (BP) and vaccine antigens, PT and FHA, on day 17 following the initial exposure (Figure 6B-D). We found that pertussis infection induced significantly higher anti-Bp IgG compared to both vaccination groups. In comparison, aP vaccinated animals exhibited significantly higher anti-PT IgG titers compared to the infection, while both aP and infection groups

showed significantly higher anti-FHA serum IgG levels compared to wP vaccination. These differences became more pronounced following three doses of vaccination. At day 17 after the final dose, wP vaccinated animals exhibited significantly higher anti-Bp IgG, whereas aP vaccinated animals showed significantly higher anti-FHA IgG, with comparable anti-PT IgG levels observed between the two vaccination groups (Figure 6E-G). Notably, antibody titers declined in both the aP and wP groups after the second vaccine dose, suggesting that the third dose was important for restoring and maintaining high antibody titers.

wP vaccination and infection elicit stronger pertussis-specific T helper responses than aP vaccination.

We evaluated the immune responses following initial exposure to aP and wP vaccines, which contain not only pertussis antigens but also matched antigen components including inactivated poliovirus, diphtheria toxoid, tetanus toxoid, and *H. influenzae* type b PRP conjugate. To specifically assess pertussis specific immune responses, we collected PBMCs at day 17 following the third dose of aP or wP vaccination, as well as from naive animals at day 14 following pertussis challenge. After stimulating with heat-killed *B. pertussis* (HKBp), we measured the cytokine production from the PBMCs associated with T helper cell polarization (Figure 7). With the strong antiviral sensing and Th1 skewed transcriptional signatures observed in aP vaccinated animals, elevated IFN-γ production was detected in their PBMCs upon HKBp stimulation (Figure 7A). However, this response was significantly lower compared to wP and infection groups indicating robust pertussis specific Th1 memory responses in these groups as well. Consistent with transcriptional signatures of Th17 activation in the wP and infection groups, both groups also exhibited significantly higher production of IL-17A and IL-17F following HKBp stimulation (Figure 7C and D). Furthermore, in line with the significant upregulations of *GATA3* and *IL4R*, both wP and infection groups showed significantly higher IL-4 production compared to aP (Figure 7E). The productions of IL-13 and TNF-α were elevated in all groups compared to their unstimulated controls but were not different between the groups (Figure 7B and F). Collectively, these data demonstrate that wP vaccination and natural infection elicit stronger and broader pertussis-specific T helper responses compared to aP vaccination, despite the latter showing prominent early innate and transcriptional activation signatures.

DISCUSSION

Leveraging a large cohort of baboons vaccinated with commercial multivalent aP or wP vaccines, or immunized by pertussis infection, we characterized early transcriptional changes following the first immunization and compared responses across the three exposure groups. Where available, we validated the identified transcriptional differences with cell differentials, cytokine profiles, and antibody responses in the peripheral blood. Across groups, we identified distinct innate, adaptive, regulatory, and humoral immune signatures, as well as transient hematological changes.

Our results indicate that vaccination with an IPV-containing pentavalent aP vaccine elicits robust antiviral innate signaling via viral nucleic acid PRRs, leading to amplification of type I IFN signaling and significant upregulation of ISGs (Figure 3B). A recent study reported that an IPV containing Tdap booster vaccine elicited strong antiviral responses in healthy adults compared with Tdap alone regardless of prior pertussis vaccination history[78]. Here, we extend these findings by demonstrating a similar response in infant baboons during primary immunization, that may have a greater impact by imprinting vaccination-induced adaptive immunity. These antiviral responses were not prominent in wP vaccinated animals even though IPV was administered at the same time and site as a separate injection. This difference may reflect the strong innate immune activation induced by the broad array of antigens and PAMPs present in the whole cell vaccine. In addition, the lack of physical coformulation could also limit the engagement of coordinated PRR and signal integration at the same site and time. Motivated by this observation, future analysis using these samples could further compare the impact of multivalent DTaP and DTwP on the immune responses to other shared vaccine components, although this question is beyond the scope of the present study.

In the absence of antiviral signaling, neither the wP nor the infection group exhibited significant upregulation of ISGs or cytotoxic granule protein genes (Figure 3B and 3C). In contrast, aP vaccinated animals showed significant upregulation of *TLR3* and *TLR7*. Only a modest increase in other TLRs was observed across all three exposure groups. Notably, we detected upregulation of CLRs in the infected animals that was absent in both vaccine groups. This included significant increases in *CLEC4D* and *CLEC5A*. In addition, notable increases in *CLEC4E* (Mincle) and *CLEC6A* (Dectin-2) were observed, although they did not reach statistical significance (Figure 4A). CLRs, primarily expressed by myeloid cells, bind carbohydrate structures and play key roles in recognizing PAMPs as well as DAMPs released from dying cells[79]. Upon ligand engagement, CLRs function not only as antigen uptake receptors that facilitate antigen presentation but also activate multiple signaling pathways leading to the activation of NF-κB pathway and the secretion of proinflammatory cytokines[80,81]. CLEC4D has been shown to be expressed by neutrophils, monocytes, and weakly by some dendritic cells, and can induce phagocytosis, cytokine production, and the respiratory burst[82]. Although its ligands are not fully characterized, previous studies show CLEC4D plays a non-redundant role in antimycobacterial immunity through recognition of treholose-6,6'-dimycolate (TDM), a mycobacterial cell wall glycolipid, thereby driving proinflammatory responses. CLEC4D deficiency has been associated with reduced mycobacterial uptake by pulmonary leukocytes and exacerbated pulmonary inflammation, marked by enhanced neutrophil recruitment [83]. Additionally, CLEC4D has been implicated in the resolution of inflammation during *Klebsiella pneumoniae* infection, suggesting a role in regulating neutrophil turnover in lungs[84]. CLEC5A (MDL-1) has been shown to recognize N-acetylglucosamine (GlcNAc) and N-acetylmuramic acid (MurNAc) disaccharides of bacterial cell walls [85]. It has also been implicated in the pathogenesis of aseptic inflammation, suggesting a potential role in sensing various fucosylated endogenous danger signals[86]. Mincle forms a functional heterodimer with CLEC4D and contributes to the initiation and modulation of immune responses by recognizing glycolipids from pathogens and lipids released by damaged cells[87]. Dectin-2 primarily binds high-mannose glycans on microbes and promotes strong Th17 immune responses[88,89]. Expression of only a single CLR, *CLEC7A*, was elevated in the aP group. The differential expression of PRRs, although potentially influenced by the proinflammatory cytokine milieu, may also reflect differences in antigen recognition that shape the initiation of subsequent innate and adaptive immune responses. In particular, the significant upregulation of CLRs in the infection group may

indicate enhanced recognition of carbohydrate-containing microbial structures and/or DAMPs, thereby contributing to the development of protective and durable immunity against pertussis.

Consistent with strong antiviral innate signaling, aP vaccinated animals showed significant upregulation of the Th1-lineage master transcription factor *TBX21* (T-bet)[90,91]. These animals also exhibited increased expression of *IL15RA* and *IL2RB*, which are important for NK cell and cytotoxic T differentiation, expansion, and survival. Despite the absence of clear T-bet induction, wP vaccinated animals exhibited significant upregulation of *STAT4*, *CD27*, *CD8A* and *CD8B*, accompanied by a significant increase in serum IL-27p28 on day 3 after vaccination. These findings suggest that both pentavalent aP and wP vaccines stimulate Th1 and cytotoxic T cell associated programs (Figure 2B-D), but they appear to do so through distinct upstream mechanisms.

Pertussis infection, and to a lesser extend wP vaccination, induced strong NF-κB activation and Th17 polarization followed by recruitment and activation of neutrophils (Figure 3B-E). However, the strong inductions of the inflammatory alarmins *S100A8*, *S100A9*, and *S100A12* were predominantly observed in infected animals (Figure 4B). These molecules exhibit antimicrobial activity by restricting the bioavailability of transition metals[92,93], and act as innate immune modulators primarily expressed by neutrophils, but also by many other myeloid cells[94]. Their signaling leads to potent chemoattraction for monocytes, macrophages, and neutrophils, and can amplify the inflammatory feedback loops by acting as DAMPs through TLR4 and the receptor for advanced glycation end products (RAGE), thereby promoting NF-κB activation, proinflammatory cytokine production, and the release of reactive oxygen species[95,96]. These observations suggest that S100 alarmins may contribute to reinforcing Th17-neutrophil feedback circuits during infection.

In this study, both aP and wP vaccines were formulated with aluminum phosphates as the adjuvant. However, canonical alum associated innate signatures including inflammasome activation and IL-33 alarmin production were observed only in the aP group (Figure 5A). Despite the absence of these innate signatures, transcriptional evidence of type 2 immunity was detected across all groups, with significant elevation of *IL4R* and *GATA3* expression in the wP and infection groups suggesting that Th2 differentiation can also arise through antigen-driven adaptive immune responses independent of the canonical alum-induced pathway. Supporting this interpretation, antigen restimulation of PBMCs isolated from animals in each immunization group induced significant production of IL-4 and IL-13 compared to unstimulated controls (Figure 7E and 7F). Furthermore, PBMCs from wP vaccinated and infected animals produced significantly more IL-4 than those from aP vaccinated animals following stimulation (Figure 7E). Together with the strong activation of NF-κB and Th17 responses in these groups, the Th2 activations in wP vaccinated and infected animals may arise as part of a broader inflammatory responses rather than through a strictly regulated Th2-biased polarization program.

Th2 responses and eosinophils are classically associated with allergenic inflammation. A recent published retrospective case-control study of Australian children born between 1997 and 1999, during the transition from wP to aP containing vaccines in Australia, suggest that infants who received wP vaccines were less likely to be diagnosed with food allergy in childhood than contemporaneous children who received aP vaccines[97]. Another recent study examining up to 3,000 infants vaccinated with either hexavalent DTaP-Hib-HepB-IPV (Infanrix, GSK) or pentavalent DTwP-Hib-HepB (Pantabio, PT Bio Farma) failed to find confirming immunological evidence of an attenuating effect of wP doses on IgE induction[98]. In our dataset, we observed elevated total IgE production during the first dose of aP or wP vaccination, as well as during pertussis infection likely reflecting the overall immune activation and pertussis toxin activity[56,57]. However, elevated total IgE was also observed following the primary series of aP vaccination, consistent with prior observations in children vaccinated with a trivalent DTaP vaccine[99]. A limitation of the study is that a trivalent DTaP vaccine was not included, preventing direct comparison of the ability of pentavalent verses trivalent aP formulations to induce serum IgE. It remains plausible that inclusion of the IPV component in modern multivalent aP vaccines alters immune polarization relative to earlier DTaP only formulations.

Our peripheral transcriptional analysis highlights the complexity of immune activations and regulations following multicomponent vaccinations and infection. Interpretation of these responses is further complicated by differences between the site of vaccination and the respiratory site of infection, as well as by the challenge of determining how immune responses to the multicomponent vaccination translate into responses in its individual antigens and their respective roles in protective immunity against the infection. Nevertheless, our data suggest that pentavalent aP vaccination elicits Th1 and Th2 associated T helper responses, broadly consistent with prior reports for trivalent aP vaccines, while also highlighting the potential adjuvanticity of the IPV component in the formulation. This feature should be considered in future studies evaluating immune responses to current commercial aP vaccines. In contrast, pentavalent wP vaccination and infection elicited detectable Th1, Th2, and Th17 responses, with Th17 responses dominating. PBMC restimulation further suggested stronger pertussis-specific responses cross Th groups in the wP and infection group compared to the aP group.

These differences in T helper responses were accompanied by distinct regulatory immune signatures. We observed stronger innate regulatory signals in the wP and infection groups, whereas the aP group showed evidence of regulatory T cell activity, marked by upregulation of FOXP3. Additionally, aP vaccination was associated with erythropoietic complement, and coagulation associated signatures, although no adverse outcomes were observed in the animals studies. One possible explanation is that, in the absence of robust proinflammatory signaling, aP induced immune responses are more tightly regulated, potentially limiting amplification. Under such conditions, systemic resources may be preferentially allocated toward homeostatic processes such as erythropoiesis.

Distinct humoral immune responses were also observed across groups. The aP group showed strong gene signatures associated with plasma cell differentiation, survival, and antibody secretion, whereas the infection group showed signatures associated with germinal center and memory B cell activation. The wP group exhibited a more balanced profile of plasma cell differentiation and memory B cell commitment. These findings warrant further investigation, and ongoing analyses will examine differences in GC activation using lymph node biopsy samples collected following vaccination.

Collectively, these results suggest that current multivalent aP vaccines induce immune signatures that may be distinct from those historically associated with trivalent DTaP formulations, likely due in part to the inclusion of the IPV component. In the absence of well-defined correlates of protection, the clinical implications of these differences remain uncertain. Notably, immune responses in the wP group more closely resembled those observed during infection,

although at lower magnitude, which may help explain why wP vaccination provides more infection-like immunity yet still does not confer sterilizing protection in the baboon model.

Recently, controlled human infection models (CHIMs) with *B. pertussis* have been developed in Europe[100] and North America[101]. Both models successfully established transient nasopharyngeal colonization, and mild symptoms observed in the North America model likely attributable to pertussis providing the opportunity to study pertussis infection in humans in a controlled setting. In these otherwise healthy adult subjects, immune responses were detected primarily with nasal swab samples collected at the site of infection, whereas systemic responses were modest and consisted largely of antibody responses[102]. These findings underscore the importance of mucosal immunity against pertussis and illustrate the utiliy of the models. However, safety considerations limit the ability of pertussis CHIMs to reproduce robust infection, study severe symptomatic disease, and follow disease through its entire progression and resolution. The baboon model therefore remains an essential complementary resource for studying pertussis pathogenesis and characterizing host immune responses to pertussis vaccination and disease. Many aspects of the current findings remain to be further investigated. Nevertheless, this study provides a framework for a more comprehensive understanding of the immune response elicited by these pertussis immunization strategies and establishes a foundation for the accompanying study examining the durability of the vaccine and infection induced immunity.

METHODS

Animals

Twenty four baboons were vaccinated at 2, 4, and 6 months of age by the subcutaneous route on the inner mid-thigh of both legs. Twelve were vaccinated with the full human dose of the commercial multivalent aP vaccine, Pentacel (Sanofi Pasteur Limited, Toronto, Canada), twelve were vaccinated with the full human dose of the commercial multivalent wP vaccine, Pentavac (Serum Institute of India, Pune, India) and the full human dose of the commercial inactivated polio vaccine, IPOL (Sanofi Pasteur Limited, Toronto, Canada) (Table 1). Nine unvaccinated animals were challenged with 10^8 to 10^9 CFUs of *B. pertussis* strain D420 at 10 months of age as previously described[3]. Procedures on the vaccinated animals were performed at Michael E Keeling Center for Comparative Medicine and Research at the University of Texas MD Anderson Cancer Center (Bastrop, TX) (protocol number 00002041-RN00). Procedures on the challenged animals were performed at the Food and Drug Administration (Silver Spring, MD) (protocol number 2009-19). All laboratories are accredited by the Association for Assessment and Accreditation of Laboratory Animal Care International in accordance with protocols approved by the Animal Care and Use Committee and the principles outlined in the *Guide for the Care and Use of Laboratory Animals* by the Institute for Laboratory Animal Resources, National Research Council[103].

Evaluation of animals

Whole blood samples were collected in BD Vacutainer® EDTA, Heparin, Serum Separation tubes, or PAXgene® Blood RNA tubes (BD Biosciences, Franklin Lake, NJ, USA) before and after vaccinations or infection as shown in Figure 1, with no more than 1% of body weight in one week or 2% in any 28-day period. All procedures were performed while the animals were anesthetized using 10 mg/kg ketamine intramuscularly.

RNA-sequencing from whole blood

RNA extraction, library preparation, and sequencing were performed at Maryland Genomics (https://marylandgenomics.org/). Blood samples were stored in PAXgene® tubes before being extracted for RNA using the standard PAXgene® Blood RNA Kit (IVD) following manufacturer's protocol (Qiagen, Venlo, Netherlands). In order to minimize ribosomal RNA background, samples were enriched for mRNA containing poly-A tails using the bead-based enrichment kit, NEBNext® Poly(A) mRNA Magnetic Isolation Module (New England Biolabs, Ipswich, MA) according to the manufacture's protocol. Enriched poly-A RNA was used to create strand-specific, dual unique indexed libraries using the NEBNext® Ultra™ II Directional RNA Library Prep Kit for Illumina® (New England Biolabs, Ipswich, MA). Manufacturer protocol was modified by diluting adapter 1:30 and using 3 ul of this dilution. Size selection of the library was performed using SPRI-select beads (Beckman Coulter Genomics, Danvers, MA). Glycosylase digestion of adapter and 2nd strand was done in the same reaction at the final amplification. A Revvity GX Touch (Waltham, MA) was utilized to assess libraries for size and quantity. The libraries were pooled, assessed by qPCR using the KAPA Library Quantification Kit (Complete, Universal) (Kapa Biosystems, Woburn, MA) and sequenced on an Illumina NovaSeq 6000 using 100bp PE reads (Illumina, San Diego, CA). Raw sequence data are deposited in NCBI BioProject PRJNA1538066.

RNA-sequencing data analysis

Alignment

Raw FASTQ files were assessed with FastQC (v0.12.0) for quality before trimmed and mapped to the baboon reference genome assembly Panubis1.0 (GCA_008728515.1) (release 109) from Ensembl using HISAT2 (v2.2.1) to obtain gene counts per sample.

Data processing and differential gene expression analysis

Gene-level raw counts were analyzed in R (v4.5.2) using edgeR (v4.6.3) and limma (v3.64.3) packages. Briefly, lowly expression genes were filtered before normalized for library size and compositional bias using the Trimmed Mean of M-values (TMM) method. For differential expression analysis, mean-variance relationships were modeled using voom with sample-specific quality weights[104,105]. Differential gene expression (DGE) was assessed using linear models including fixed effects for experimental group, batch, and sex implemented in limma. To account for repeated measures within animals, intra-animal correlation was estimated using the duplicateCorrelation function[106]. To compare between groups or time points, pre-specified contrasts were constructed with contrast-specific statistics computed followed by empirical Bayes moderation to stabilize variance estimates across genes. DGE results were extracted

using the topTable function in limma. All statistical tests were adjusted for multiple comparisons using the Benjamini-Hochberg false discovery rate (FDR) method. Genes with FDR-adjusted p-values below the prespecified threshold were considered statistically significant. DGE models were fitted using baboon Ensembl gene identifiers, and baboon-specific annotations were used for Gene Ontology pathway analyses. For downstream analyses and biological interpretation, baboon Ensembl gene identifiers were mapped to human orthologous gene symbols using biomaRt (v2.64.0) package with Ensembl database. Where multiple mapping occurred, a single representative gene was retained based on highest average expression across samples. Baboon-to-human orthology mapping was performed only after DGE analysis and therefore did not affect read alignment, expression quantification, fold-change estimation, or statistical testing. Human ortholog symbols were added solety to facilitate functional annotation and biological interpretation. Among the genes retained after low-expression filtering, 86.2% had a matched human ortholog. For genes without an identified human ortholog, the original baboon Ensembl identifiers were retained. All gene sympols displayed in the main figures were manually verified.

Weighted gene co-expression network analysis

Batch-corrected log2 counts per million (CPM) were filtered to retain approximately 9000 genes that are within the top 60% of variance across samples prior to unsupervised weighted gene co-expression network analysis (WGCNA) using WGCNA (v1.74) package. A signed network was constructed with a soft-thresholding power of 5, selected as the minimum power achieving a scale-free topology fit index (R^2) ³ 0.8. Modules were identified using dynamic tree cutting with a minimum module size of 20 genes and merged based on eigengene similarity. Module eigengenes (MEs), defined as the first principal component of each module, were extracted and used for downstream analysis. Within each group, longitudinal changes relative to baseline were assessed using paired Wilcoxon signed-rank tests accounting for repeated measures within the same animal. Functional enrichment analysis was conducted for genes within each module using over-representation analysis with the enricher function from clusterProfiler (v4.16.0). Gene Ontology (GO) terms were retrieved from the baboon Ensembl dataset via the biomaRt package. Multiple testing correction was performed using the Benjamini-Hochberg FDR method. Terms with FDR < 0.05 were considered significant.

Pathway analysis

Gene set enrichment analysis (GSEA) was performed separately for each group. For each time point, differential expression relative to baseline was calculated and ranked prior to GSEA using the GSEA function from clusterProfiler package against GO terms. Over-representation analysis was conducted using enricher function from clusterProfiler package against GO terms. Multiple testing correction was performed using the Benjamini-Hochberg FDR method. Terms with FDR < 0.05 were considered significant. Source code for the RNA sequencing analysis is publicly available at https://github.com/yhw723/pertussis_immune_profiling.

Detection of Antibody Titers

Serum samples were assessed for pertussis-specific immunoglobulin (Ig) G levels using an enzyme-linked immunosorbent assay (ELISA). First, Nunc 96-well plates were coated with 0.2 ug/mL pertussis toxin (PT) (List Labs, Campbell, CA), 0.5 ug/mL filamentous hemagglutinin adhesin (FHA) (Enzo, Farmingdale, NY), or HKBp at an optical density of 0.9 at 600 nm overnight at 4°C. Following blocking nonspecific binding with 1% bovine serum albumin in PBS for 2 hours, serial diluted samples were added and incubated for 1 hour at room temperature. Bound antibodies were detected using horseradish peroxidase (HRP)-conjugated mouse anti-monkey IgG antibody (Bio-Rad, Hercules, CA) followed by KPL SureBlue TMB Microwell peroxidase substrate (Seracare, Milford, MA). Optical densities were read at 450 nm with a Molecular devices VERSA Max microplate reader and analyzed using SoftMax Pro software (v7.1.2). With each plate, a standard curve was included, using World Health Organization (WHO) international pertussis antiserum (National Institute for Biological Standards and Control). IgG results were expressed as international units per milliliter (IU/mL) by comparing the results with the linear portion of the standard curve.

For total IgE levels, anti-human IgE antibody (Bethyl, Montgomery, TX) were used as coating antibodies. After blocking for nonspecific binding, bound antibodies from serum were detected using HRP-conjugated goat anti-human IgE antibody (Bethyl). Total IgE results were expressed as relative unites per milliliter (RU/mL) by comparing the results with the linear portion of the standard curve of a positive control.

PBMC restimulations

Whole blood was collected into blood tubes with EDTA (Biosciences) before layered over the Histopaque-1077 solution (Sigma-Aldrich, Burlington, MA) and centrifuged at 400 x g for 30 minutes at room temperature to separate PBMCs. Heat-killed *B.pertussis* (HKBp) was prepared by heat-inactivating *B.pertussis* D420 cells suspended in PBS at OD600 0.9 for 30 min at 65°C. PBMCs were resuspended at 5 x 10^6 cells/mL in Roswell Park Memorial Institute (RPMI) 1640 medium (Gibco) supplemented with 10% heat-inactivated FBS (Gibco), 1% 100x Antibiotic/Antimycotic Solution (Gibco), 1% L-glutamine (Gibco) and 25 mM HEPES (Sigma-Aldrich) (complete RPMI). The cells were incubated with or without HKBp (50 bacteria per PBMC) at 37°C. Supernatants were collected after 72 h.

Detection of Cytokine Production

For the analysis of cytokine production of IL-13, IL-6, IFN-γ, TNF-α, IL-17A, IL-17F, and IL-4 in baboon serum or restimulated PBMC supernatant, a bead-based immunoassay LEGENDplex HU Th Cytokine Panel V02 (BioLegend, San Diego, CA) was used, according to manufacturer instructions. Data acquisition was performed on LSRFortessa X-20 flow cytometer (BD Biosciences) using Diva software (BD Biosciences) and analyzed using LEGENDplex Data Analysis Software Suite (BioLegend). 3

Baboon serum samples were also assessed for GM-CSF, IL-27p28 and IL-23 protein levels using ELISA (U-CyTech, Netherlands), following the manufacturer's instructions. First, 96-well plates were coated with anti-monkey or anti-human polyclonal antibody for specific cytokines at 4°C overnight. Following blocking

nonspecific binding with 1% bovine serum albumin in 1× PBS for 2 hours, samples and recombinant standards for the respective cytokine were added and incubated for 2 hours at 37°C. Bound cytokine was detected using cytokine-specific biotinylated monoclonal antibody and streptavidin–horseradish peroxidase, followed by KPL SureBlue TMB Microwell peroxidase substrate (Seracare). Optical densities were read at 450 nm with a Molecular devices VERSA Max microplate reader and analyzed using SoftMax Pro software (v7.1.2).

Quantification and Statistical Analysis

All statistical analyses were performed using R (v4.5.2). Comparisons between independent groups were conducted using the unpaired Mann–Whitney U test. Comparisons between time points within each group were performed using the paired Wilcoxon signed-rank test. Associations between variables were assessed using Pearson's correlation coefficient. Statistical significance and correlation coefficients are reported in the corresponding figures.

Declarations

RESOURCE AVAILABILITY

Lead contact

Requests for further information and resources should be directed to and will be fulfilled by the lead contact, Yihui Wang (yihui.wang@fda.hhs.gov).

Materials availability

This study did not generate new unique reagents.

Data and code availability

All sequencing data and code are deposited and available from public archives.

Clinical trial number

Not applicable.

ACKNOWLEDGMENTS

Research reported in this publication was supported by the internal FDA research budget and by NIH/FDA Interagency Agreement (AAI23046-001-00000, AAI22039-001-00000, and AAI20045-001-00000). The project was also supported in part by the NIH under award number P40OD024628 (SPF Baboon Research Resource).

AUTHOR CONTRIBUTIONS

Conceptualization, T.M. and Y.W.; methodology, T.M. and Y.W; Investigation, Y.W. and J.M.; writing – original draft, Y.W.; writing – review & editing, T.M. and J.M.; funding acquisition, T.M.; supervision, T.M.

DECLARATION OF INTERESTS

The authors have no conflicts of interest.

References

1. Scruggs-Wodkowski, E. & Malani, P. What Is Pertussis? *JAMA* 332, 1030–1030 (2024). https://doi.org/10.1001/jama.2024.9049
2. Warfel, J. M., Beren, J. & Merkel, T. J. Airborne transmission of Bordetella pertussis. *J Infect Dis* 206, 902–906 (2012). https://doi.org/10.1093/infdis/jis443
3. Kapil, P., Wang, Y., Zimmerman, L., Gaykema, M. & Merkel, T. J. Repeated Bordetella pertussis Infections Are Required to Reprogram Acellular Pertussis Vaccine-Primed Host Responses in the Baboon Model. *J Infect Dis* 229, 376–383 (2024). https://doi.org/10.1093/infdis/jiad332
4. *New and Nonofficial Remedies*. Vol. 1914 247 (American Medical Association, 1914).
5. Cherry, J. D., Brunell, P. A., Golden, G. S. & Karzon, D. T. Report of the Task Force on Pertussis and Pertussis Immunization—1988. *Pediatrics* 81, 933–984 (1988). https://doi.org/10.1542/peds.81.6.933

6. Gustafsson, L., Hallander, H. O., Olin, P., Reizenstein, E. & Storsaeter, J. A controlled trial of a two-component acellular, a five-component acellular, and a whole-cell pertussis vaccine. *N Engl J Med* 334, 349–355 (1996). https://doi.org/10.1056/NEJM199602083340602
7. Greco, D. *et al.* A controlled trial of two acellular vaccines and one whole-cell vaccine against pertussis. Progetto Pertosse Working Group. *N Engl J Med* 334, 341–348 (1996). https://doi.org/10.1056/NEJM199602083340601
8. Olin, P., Rasmussen, F., Gustafsson, L., Hallander, H. O. & Heijbel, H. Randomised controlled trial of two-component, three-component, and five-component acellular pertussis vaccines compared with whole-cell pertussis vaccine. Ad Hoc Group for the Study of Pertussis Vaccines. *Lancet* 350, 1569–1577 (1997). https://doi.org/10.1016/s0140-6736(97)06508-2
9. Simondon, F. *et al.* A randomized double-blind trial comparing a two-component acellular to a whole-cell pertussis vaccine in Senegal. *Vaccine* 15, 1606–1612 (1997). https://doi.org/10.1016/s0264-410x(97)00100-x
10. Trollfors, B. *et al.* A placebo-controlled trial of a pertussis-toxoid vaccine. *N Engl J Med* 333, 1045–1050 (1995). https://doi.org/10.1056/NEJM199510193331604
11. ReportLinker. *A White Paper To Understand The Market Structure Of Pediatric Pertussis Hexavalent and Combination Vaccines*, %3Chttps://ai.reportlinker.com/hubfs/Sanofi/A%20White%20Paper%20To%20UnderstandTheMarketStructure%20Of%20Pediatric%20PertussisHexavaler (2024).
12. UNICEF. *Diphtheria Tetanus and Pertussis Containing Vaccines: Market and Supply Update*, <https://www.unicef.org/supply/media/17606/file/Diphtheria-Tetanus-Pertussis-Vaccine-Containing-Market-and-Supply-Update-June-2023.pdf%3E (2023).
13. ChildVaxView. *Vaccination Coverage among Young Children (0–35 Months)*, %3Chttps://www.cdc.gov/childvaxview/about/interactive-reports.html%3E (
14. CDC. *Pertussis Surveillance and Trends*, %3Chttps://www.cdc.gov/pertussis/php/surveillance/index.html%3E (2025).
15. CDC. *Pertussis Cases by Year (1922–2023)*, %3Chttps://www.cdc.gov/pertussis/php/surveillance/pertussis-cases-by-year.html%3E (
16. Althouse, B. M. & Scarpino, S. V. Asymptomatic transmission and the resurgence of Bordetella pertussis. *BMC Med* 13, 146 (2015). https://doi.org/10.1186/s12916-015-0382-8
17. Warfel, J. M., Zimmerman, L. I. & Merkel, T. J. Acellular pertussis vaccines protect against disease but fail to prevent infection and transmission in a nonhuman primate model. *Proc Natl Acad Sci U S A* 111, 787–792 (2014). https://doi.org/10.1073/pnas.1314688110
18. Plotkin, S. A. The Pertussis Problem. *Clinical Infectious Diseases* 58, 830–833 (2013). https://doi.org/10.1093/cid/cit934
19. Storsaeter, J., Hallander, H. O., Gustafsson, L. & Olin, P. Levels of anti-pertussis antibodies related to protection after household exposure to Bordetella pertussis. *Vaccine* 16, 1907–1916 (1998). https://doi.org/10.1016/s0264-410x(98)00227-8
20. Ausiello, C. M. *et al.* Cell-mediated immune responses in four-year-old children after primary immunization with acellular pertussis vaccines. *Infect Immun* 67, 4064–4071 (1999). https://doi.org/10.1128/IAI.67.8.4064-4071.1999
21. Ryan, M., Gothefors, L., Storsaeter, J. & Mills, K. H. Bordetella pertussis-specific Th1/Th2 cells generated following respiratory infection or immunization with an acellular vaccine: comparison of the T cell cytokine profiles in infants and mice. *Dev Biol Stand* 89, 297–305 (1997).
22. Ross, P. J. *et al.* Relative contribution of Th1 and Th17 cells in adaptive immunity to Bordetella pertussis: towards the rational design of an improved acellular pertussis vaccine. *PLoS Pathog* 9, e1003264 (2013). https://doi.org/10.1371/journal.ppat.1003264
23. Borkner, L., Curham, L. M., Wilk, M. M., Moran, B. & Mills, K. H. G. IL-17 mediates protective immunity against nasal infection with Bordetella pertussis by mobilizing neutrophils, especially Siglec-F(+) neutrophils. *Mucosal Immunol* (2021). https://doi.org/10.1038/s41385-021-00407-5
24. Misiak, A., Wilk, M. M., Raverdeau, M. & Mills, K. H. IL-17-Producing Innate and Pathogen-Specific Tissue Resident Memory gammadelta T Cells Expand in the Lungs of Bordetella pertussis-Infected Mice. *J Immunol* 198, 363–374 (2017). https://doi.org/10.4049/jimmunol.1601024
25. Wilk, M. M. *et al.* Immunization with whole cell but not acellular pertussis vaccines primes CD4 TRM cells that sustain protective immunity against nasal colonization with Bordetella pertussis. *Emerg Microbes Infect* 8, 169–185 (2019). https://doi.org/10.1080/22221751.2018.1564630
26. Ausiello, C. M., Urbani, F., la Sala, A., Lande, R. & Cassone, A. Vaccine- and antigen-dependent type 1 and type 2 cytokine induction after primary vaccination of infants with whole-cell or acellular pertussis vaccines. *Infect Immun* 65, 2168–2174 (1997). https://doi.org/10.1128/iai.65.6.2168-2174.1997
27. Durinck, S. *et al.* BioMart and Bioconductor: a powerful link between biological databases and microarray data analysis. *Bioinformatics* 21, 3439–3440 (2005). https://doi.org/10.1093/bioinformatics/bti525
28. Subramanian, A. *et al.* Gene set enrichment analysis: a knowledge-based approach for interpreting genome-wide expression profiles. *Proc Natl Acad Sci U S A* 102, 15545–15550 (2005). https://doi.org/10.1073/pnas.0506580102
29. Zhang, B. & Horvath, S. A general framework for weighted gene co-expression network analysis. *Stat Appl Genet Mol Biol* 4, Article17 (2005). https://doi.org/10.2202/1544-6115.1128
30. da Silva Antunes, R. *et al.* A system-view of Bordetella pertussis booster vaccine responses in adults primed with whole-cell versus acellular vaccine in infancy. *JCI Insight* 6 (2021). https://doi.org/10.1172/jci.insight.141023
31. Inkeles, M. S. *et al.* Cell-type deconvolution with immune pathways identifies gene networks of host defense and immunopathology in leprosy. *JCI Insight* 1, e88843 (2016). https://doi.org/10.1172/jci.insight.88843
32. Rehwinkel, J. & Gack, M. U. RIG-I-like receptors: their regulation and roles in RNA sensing. *Nat Rev Immunol* 20, 537–551 (2020). https://doi.org/10.1038/s41577-020-0288-3
33. Miyashita, M., Oshiumi, H., Matsumoto, M. & Seya, T. DDX60, a DEXD/H box helicase, is a novel antiviral factor promoting RIG-I-like receptor-mediated signaling. *Mol Cell Biol* 31, 3802–3819 (2011). https://doi.org/10.1128/MCB.01368-10

34. Schneider, W. M., Chevillotte, M. D. & Rice, C. M. Interferon-stimulated genes: a complex web of host defenses. *Annu Rev Immunol* 32, 513–545 (2014). https://doi.org/10.1146/annurev-immunol-032713-120231
35. Zhu, J., Yamane, H. & Paul, W. E. Differentiation of effector CD4 T cell populations (*). *Annu Rev Immunol* 28, 445–489 (2010). https://doi.org/10.1146/annurev-immunol-030409-101212
36. Iwasaki, Y., Fujio, K., Okamura, T. & Yamamoto, K. Interleukin-27 in T cell immunity. *Int J Mol Sci* 16, 2851–2863 (2015). https://doi.org/10.3390/ijms16022851
37. Yoshida, H. & Hunter, C. A. The immunobiology of interleukin-27. *Annu Rev Immunol* 33, 417–443 (2015). https://doi.org/10.1146/annurev-immunol-032414-112134
38. Turiello, R. *et al.* NKG7 is a Stable Marker of Cytotoxicity Across Immune Contexts and Within the Tumor Microenvironment. *Eur J Immunol* 55, e51885 (2025). https://doi.org/10.1002/eji.202551885
39. Abel, A. M., Yang, C., Thakar, M. S. & Malarkannan, S. Natural Killer Cells: Development, Maturation, and Clinical Utilization. *Front Immunol* 9, 1869 (2018). https://doi.org/10.3389/fimmu.2018.01869
40. Reis e Sousa, C., Yamasaki, S. & Brown, G. D. Myeloid C-type lectin receptors in innate immune recognition. *Immunity* 57, 700–717 (2024). https://doi.org/10.1016/j.immuni.2024.03.005
41. Shiokawa, M., Yamasaki, S. & Saijo, S. C-type lectin receptors in anti-fungal immunity. *Curr Opin Microbiol* 40, 123–130 (2017). https://doi.org/10.1016/j.mib.2017.11.004
42. Solt, L. A. & Burris, T. P. Action of RORs and their ligands in (patho)physiology. *Trends Endocrinol Metab* 23, 619–627 (2012). https://doi.org/10.1016/j.tem.2012.05.012
43. Kanno, T., Nakano, K. & Endo, Y. Cellular metabolism in Th9, Th17, and Treg cell differentiation. *Int Immunol* 37, 673–682 (2025). https://doi.org/10.1093/intimm/dxaf032
44. Ciofani, M. *et al.* A validated regulatory network for Th17 cell specification. *Cell* 151, 289–303 (2012). https://doi.org/10.1016/j.cell.2012.09.016
45. Korn, T., Bettelli, E., Oukka, M. & Kuchroo, V. K. IL-17 and Th17 Cells. *Annu Rev Immunol* 27, 485–517 (2009). https://doi.org/10.1146/annurev.immunol.021908.132710
46. Cordero, H. Chemokine receptors in primary and secondary lymphoid tissues. *Int Rev Cell Mol Biol* 388, 1–19 (2024). https://doi.org/10.1016/bs.ircmb.2023.11.003
47. Mills, K. H. G. IL-17 and IL-17-producing cells in protection versus pathology. *Nat Rev Immunol* 23, 38–54 (2023). https://doi.org/10.1038/s41577-022-00746-9
48. Ehrchen, J. M., Sunderkotter, C., Foell, D., Vogl, T. & Roth, J. The endogenous Toll-like receptor 4 agonist S100A8/S100A9 (calprotectin) as innate amplifier of infection, autoimmunity, and cancer. *J Leukoc Biol* 86, 557–566 (2009). https://doi.org/10.1189/jlb.1008647
49. Zheng, C. *et al.* Dual role of CD177 + neutrophils in inflammatory bowel disease: a review. *J Transl Med* 22, 813 (2024). https://doi.org/10.1186/s12967-024-05539-3
50. Lawrence, S. M., Corriden, R. & Nizet, V. The Ontogeny of a Neutrophil: Mechanisms of Granulopoiesis and Homeostasis. *Microbiol Mol Biol Rev* 82 (2018). https://doi.org/10.1128/MMBR.00057-17
51. Eisenbarth, S. C., Colegio, O. R., O'Connor, W., Sutterwala, F. S. & Flavell, R. A. Crucial role for the Nalp3 inflammasome in the immunostimulatory properties of aluminium adjuvants. *Nature* 453, 1122–1126 (2008). https://doi.org/10.1038/nature06939
52. Pulendran, B., P, S. A. & O'Hagan, D. T. Emerging concepts in the science of vaccine adjuvants. *Nat Rev Drug Discov* 20, 454–475 (2021). https://doi.org/10.1038/s41573-021-00163-y
53. Rose, W. A., 2nd, Okragly, A. J., Patel, C. N. & Benschop, R. J. IL-33 released by alum is responsible for early cytokine production and has adjuvant properties. *Sci Rep* 5, 13146 (2015). https://doi.org/10.1038/srep13146
54. Bochner, B. S. & Gleich, G. J. What targeting eosinophils has taught us about their role in diseases. *J Allergy Clin Immunol* 126, 16–25; quiz 26 – 17 (2010). https://doi.org/10.1016/j.jaci.2010.02.026
55. Snodgrass, R. G. & Brune, B. Regulation and Functions of 15-Lipoxygenases in Human Macrophages. *Front Pharmacol* 10, 719 (2019). https://doi.org/10.3389/fphar.2019.00719
56. Munoz, J. J., Arai, H., Bergman, R. K. & Sadowski, P. L. Biological activities of crystalline pertussigen from Bordetella pertussis. *Infect Immun* 33, 820–826 (1981). https://doi.org/10.1128/iai.33.3.820-826.1981
57. Samore, M. H. & Siber, G. R. Pertussis toxin enhanced IgG1 and IgE responses to primary tetanus immunization are mediated by interleukin-4 and persist during secondary responses to tetanus alone. *Vaccine* 14, 290–297 (1996). https://doi.org/10.1016/0264-410x(95)00201-b
58. Ho, I. C., Tai, T. S. & Pai, S. Y. GATA3 and the T-cell lineage: essential functions before and after T-helper-2-cell differentiation. *Nat Rev Immunol* 9, 125–135 (2009). https://doi.org/10.1038/nri2476
59. Ricklin, D., Hajishengallis, G., Yang, K. & Lambris, J. D. Complement: a key system for immune surveillance and homeostasis. *Nat Immunol* 11, 785–797 (2010). https://doi.org/10.1038/ni.1923
60. Werner, L. M. & Criss, A. K. Diverse Functions of C4b-Binding Protein in Health and Disease. *J Immunol* 211, 1443–1449 (2023). https://doi.org/10.4049/jimmunol.2300333
61. de Bont, C. M., Boelens, W. C. & Pruijn, G. J. M. NETosis, complement, and coagulation: a triangular relationship. *Cell Mol Immunol* 16, 19–27 (2019). https://doi.org/10.1038/s41423-018-0024-0

62. Yong, J. & Toh, C. H. Rethinking coagulation: from enzymatic cascade and cell-based reactions to a convergent model involving innate immune activation. *Blood* 142, 2133–2145 (2023). https://doi.org/10.1182/blood.2023021166
63. Skonier, J. *et al.* beta ig-h3: a transforming growth factor-beta-responsive gene encoding a secreted protein that inhibits cell attachment in vitro and suppresses the growth of CHO cells in nude mice. *DNA Cell Biol* 13, 571–584 (1994). https://doi.org/10.1089/dna.1994.13.571
64. Hao, X. *et al.* The regulatory role and mechanism of TGFBI on Tregs in the immune microenvironment of clear cell renal cell carcinoma. *Int J Surg* 111, 9134–9146 (2025). https://doi.org/10.1097/JS9.0000000000003225
65. Molinier-Frenkel, V., Prevost-Blondel, A. & Castellano, F. The IL4I1 Enzyme: A New Player in the Immunosuppressive Tumor Microenvironment. *Cells* 8 (2019). https://doi.org/10.3390/cells8070757
66. Sadik, A. *et al.* IL4I1 Is a Metabolic Immune Checkpoint that Activates the AHR and Promotes Tumor Progression. *Cell* 182, 1252–1270 e1234 (2020). https://doi.org/10.1016/j.cell.2020.07.038
67. Nold, M. F. *et al.* IL-37 is a fundamental inhibitor of innate immunity. *Nat Immunol* 11, 1014–1022 (2010). https://doi.org/10.1038/ni.1944
68. Seo, H. *et al.* TOX and TOX2 transcription factors cooperate with NR4A transcription factors to impose CD8(+) T cell exhaustion. *Proc Natl Acad Sci U S A* 116, 12410–12415 (2019). https://doi.org/10.1073/pnas.1905675116
69. Anderson, A. C., Joller, N. & Kuchroo, V. K. Lag-3, Tim-3, and TIGIT: Co-inhibitory Receptors with Specialized Functions in Immune Regulation. *Immunity* 44, 989–1004 (2016). https://doi.org/10.1016/j.immuni.2016.05.001
70. Schuh, W., Mielenz, D. & Jack, H. M. Unraveling the mysteries of plasma cells. *Adv Immunol* 146, 57–107 (2020). https://doi.org/10.1016/bs.ai.2020.01.002
71. Andreani, V. *et al.* Cochaperone Mzb1 is a key effector of Blimp1 in plasma cell differentiation and beta1-integrin function. *Proc Natl Acad Sci U S A* 115, E9630-E9639 (2018). https://doi.org/10.1073/pnas.1809739115
72. Crotty, S. Follicular helper CD4 T cells (TFH). *Annu Rev Immunol* 29, 621–663 (2011). https://doi.org/10.1146/annurev-immunol-031210-101400
73. Smulski, C. R. & Eibel, H. BAFF and BAFF-Receptor in B Cell Selection and Survival. *Front Immunol* 9, 2285 (2018). https://doi.org/10.3389/fimmu.2018.02285
74. Davis, R. S. Fc receptor-like molecules. *Annu Rev Immunol* 25, 525–560 (2007). https://doi.org/10.1146/annurev.immunol.25.022106.141541
75. Basso, K. & Dalla-Favera, R. Roles of BCL6 in normal and transformed germinal center B cells. *Immunol Rev* 247, 172–183 (2012). https://doi.org/10.1111/j.1600-065X.2012.01112.x
76. Choi, J. & Crotty, S. Bcl6-Mediated Transcriptional Regulation of Follicular Helper T cells (T(FH)). *Trends Immunol* 42, 336–349 (2021). https://doi.org/10.1016/j.it.2021.02.002
77. Nimmerjahn, F. & Ravetch, J. V. Fcgamma receptors as regulators of immune responses. *Nat Rev Immunol* 8, 34–47 (2008). https://doi.org/10.1038/nri2206
78. Gillard, J. *et al.* Antiviral responses induced by Tdap-IPV vaccination are associated with persistent humoral immunity to Bordetella pertussis. *Nat Commun* 15, 2133 (2024). https://doi.org/10.1038/s41467-024-46560-w
79. Zhu, L. L. *et al.* C-type lectin receptors Dectin-3 and Dectin-2 form a heterodimeric pattern-recognition receptor for host defense against fungal infection. *Immunity* 39, 324–334 (2013). https://doi.org/10.1016/j.immuni.2013.05.017
80. Dambuza, I. M. & Brown, G. D. C-type lectins in immunity: recent developments. *Curr Opin Immunol* 32, 21–27 (2015). https://doi.org/10.1016/j.coi.2014.12.002
81. Robinson, M. J., Sancho, D., Slack, E. C., LeibundGut-Landmann, S. & Reis e Sousa, C. Myeloid C-type lectins in innate immunity. *Nat Immunol* 7, 1258–1265 (2006). https://doi.org/10.1038/ni1417
82. Graham, L. M. *et al.* The C-type lectin receptor CLECSF8 (CLEC4D) is expressed by myeloid cells and triggers cellular activation through Syk kinase. *J Biol Chem* 287, 25964–25974 (2012). https://doi.org/10.1074/jbc.M112.384164
83. Wilson, G. J. *et al.* The C-type lectin receptor CLECSF8/CLEC4D is a key component of anti-mycobacterial immunity. *Cell Host Microbe* 17, 252–259 (2015). https://doi.org/10.1016/j.chom.2015.01.004
84. Steichen, A. L., Binstock, B. J., Mishra, B. B. & Sharma, J. C-type lectin receptor Clec4d plays a protective role in resolution of Gram-negative pneumonia. *J Leukoc Biol* 94, 393–398 (2013). https://doi.org/10.1189/jlb.1212622
85. Chen, S. T. *et al.* CLEC5A is a critical receptor in innate immunity against Listeria infection. *Nat Commun* 8, 299 (2017). https://doi.org/10.1038/s41467-017-00356-3
86. Joyce-Shaikh, B. *et al.* Myeloid DAP12-associating lectin (MDL)-1 regulates synovial inflammation and bone erosion associated with autoimmune arthritis. *J Exp Med* 207, 579–589 (2010). https://doi.org/10.1084/jem.20090516
87. Richardson, M. B. & Williams, S. J. MCL and Mincle: C-Type Lectin Receptors That Sense Damaged Self and Pathogen-Associated Molecular Patterns. *Front Immunol* 5, 288 (2014). https://doi.org/10.3389/fimmu.2014.00288
88. Robinson, M. J. *et al.* Dectin-2 is a Syk-coupled pattern recognition receptor crucial for Th17 responses to fungal infection. *J Exp Med* 206, 2037–2051 (2009). https://doi.org/10.1084/jem.20082818
89. Saijo, S. *et al.* Dectin-2 recognition of alpha-mannans and induction of Th17 cell differentiation is essential for host defense against Candida albicans. *Immunity* 32, 681–691 (2010). https://doi.org/10.1016/j.immuni.2010.05.001
90. Braun, M. *et al.* NK cell activation in human hantavirus infection explained by virus-induced IL-15/IL15Ralpha expression. *PLoS Pathog* 10, e1004521 (2014). https://doi.org/10.1371/journal.ppat.1004521

91. Hashimoto, M., Im, S. J., Araki, K. & Ahmed, R. Cytokine-Mediated Regulation of CD8 T-Cell Responses During Acute and Chronic Viral Infection. *Cold Spring Harb Perspect Biol* 11 (2019). https://doi.org/10.1101/cshperspect.a028464
92. Kehl-Fie, T. E. *et al.* Nutrient metal sequestration by calprotectin inhibits bacterial superoxide defense, enhancing neutrophil killing of Staphylococcus aureus. *Cell Host Microbe* 10, 158–164 (2011). https://doi.org/10.1016/j.chom.2011.07.004
93. Zygiel, E. M. & Nolan, E. M. Transition Metal Sequestration by the Host-Defense Protein Calprotectin. *Annu Rev Biochem* 87, 621–643 (2018). https://doi.org/10.1146/annurev-biochem-062917-012312
94. Ryckman, C., Vandal, K., Rouleau, P., Talbot, M. & Tessier, P. A. Proinflammatory activities of S100: proteins S100A8, S100A9, and S100A8/A9 induce neutrophil chemotaxis and adhesion. *J Immunol* 170, 3233–3242 (2003). https://doi.org/10.4049/jimmunol.170.6.3233
95. Ma, L., Sun, P., Zhang, J. C., Zhang, Q. & Yao, S. L. Proinflammatory effects of S100A8/A9 via TLR4 and RAGE signaling pathways in BV-2 microglial cells. *Int J Mol Med* 40, 31–38 (2017). https://doi.org/10.3892/ijmm.2017.2987
96. Simard, J. C. *et al.* S100A8 and S100A9 induce cytokine expression and regulate the NLRP3 inflammasome via ROS-dependent activation of NF-kappaB(1.). *PLoS One* 8, e72138 (2013). https://doi.org/10.1371/journal.pone.0072138
97. Estcourt, M. J. *et al.* Whole-Cell Pertussis Vaccination and Decreased Risk of IgE-Mediated Food Allergy: A Nested Case-Control Study. *J Aller Cl Imm-Pract* 8, 2004–2014 (2020). https://doi.org/10.1016/j.jaip.2019.12.020
98. Perez Chacon, G. *et al.* Immunogenicity, reactogenicity, and IgE-mediated immune responses of a mixed whole-cell and acellular pertussis vaccine schedule in Australian infants: A randomised, double-blind, noninferiority trial. *PLoS Med* 21, e1004414 (2024). https://doi.org/10.1371/journal.pmed.1004414
99. Ryan, E. J., Nilsson, L., Kjellman, N., Gothefors, L. & Mills, K. H. Booster immunization of children with an acellular pertussis vaccine enhances Th2 cytokine production and serum IgE responses against pertussis toxin but not against common allergens. *Clin Exp Immunol* 121, 193–200 (2000). https://doi.org/10.1046/j.1365-2249.2000.01306.x
100. de Graaf, H. *et al.* Controlled Human Infection With Bordetella pertussis Induces Asymptomatic, Immunizing Colonization. *Clin Infect Dis* 71, 403–411 (2020). https://doi.org/10.1093/cid/ciz840
101. ElSherif, M. S. *et al.* A controlled human infection model for symptomatic pertussis in North America using the pertactin-producing clinical isolate D420. *medRxiv* (2026). https://doi.org/10.64898/2026.06.09.26355227
102. Willemsen, L. *et al.* Pre-existing antibodies predict protection while mucosal inflammation correlates with symptomatic Bordetella pertussis infection. *medRxiv* (2026). https://doi.org/10.64898/2026.06.26.26356067
103. *The Guide for the Care and Use of Laboratory Animals (Eighth Edition, 2011)*. (National Academies Press, 2011).
104. Law, C. W., Chen, Y., Shi, W. & Smyth, G. K. voom: Precision weights unlock linear model analysis tools for RNA-seq read counts. *Genome Biol* 15, R29 (2014). https://doi.org/10.1186/gb-2014-15-2-r29
105. Liu, R. *et al.* Why weight? Modelling sample and observational level variability improves power in RNA-seq analyses. *Nucleic Acids Res* 43, e97 (2015). https://doi.org/10.1093/nar/gkv412
106. Ritchie, M. E. *et al.* limma powers differential expression analyses for RNA-sequencing and microarray studies. *Nucleic Acids Res* 43, e47 (2015). https://doi.org/10.1093/nar/gkv007

Tables

Table 1 and 2 are available in the Supplementary Files section.

Figures

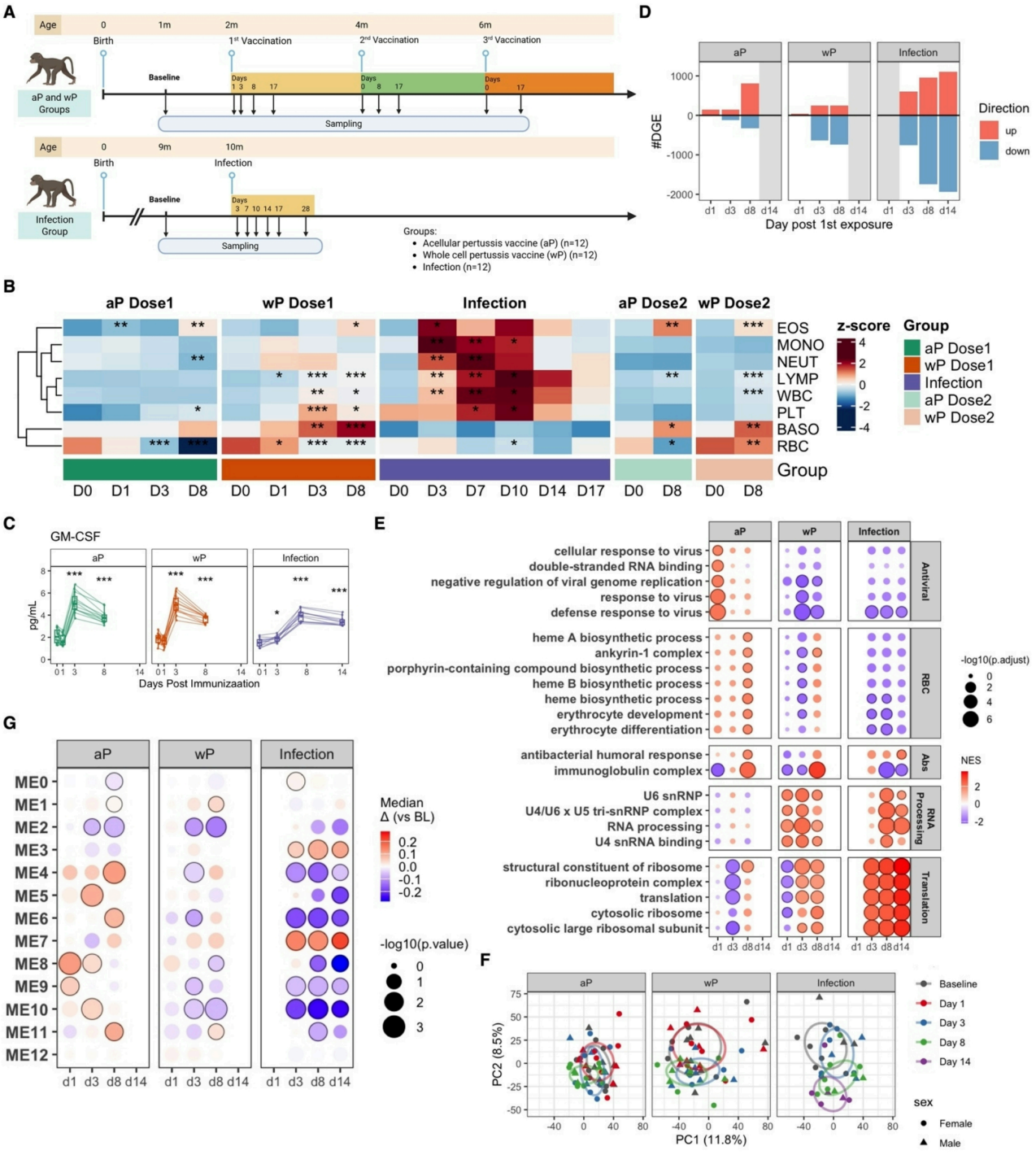


Figure 1

Distinct cellular and molecular signatures across immunization groups.

A)Study scheme. **B)** Complete blood cell counts (CBC) were measured from peripheral blood collected during vaccination (days 0, 1, 3, and 8 following the first dose, and days 0 and 8 following the second dose) and infection (days 0, 3, 7, 10, 14, and 17). Heatmaps are normalized by row and shown as *z*-score. **C)** Serum GM-CSF levels following vaccination or infection. Statistical comparisons in **B)** and **C)** were performed for each time point relative to their corresponding baseline (D0) within each group using paired Wilcoxon signed-rank test (**** P £ 0.0001, *** P £0.001, ** P £0.01, * P £0.05). **D)** Numbers of differentially expressed genes over time following initial exposure compared to the baseline of respective groups. Differential expression was defined as a fold change greater than 1.5 in either direction and FDR less than 0.05. **E)** Longitudinal pathway enrichment across treatment groups using gene set enrichment analysis. Selected pathways identified are shown across time points and treatment groups. For each time point, differential expression relative to

baseline was calculated and ranked prior to GSEA against GO terms. Color indicates normalized enrichment score (NES), size indicates -log10(FDR), and black outlines denote FDR < 0.05. Pathways are grouped by functional category and faceted by group. **F)**Principle component analysis (PCA) of gene expression profiles showing temporal changes and sex associated variation within each group. **G)** Longitudinal changes in WGCNA module eigengenes relative to baseline. For each module (ME0-ME12), paired difference in module eigengene between baseline and post-immunization time points are shown for aP, wP, and infection groups. Color represents the median and direction of paired changes. Point size corresponds to -log10(p.value) from paired Wilcoxon signed-rank tests. Black outlines indicate statistical significance (p < 0.05).

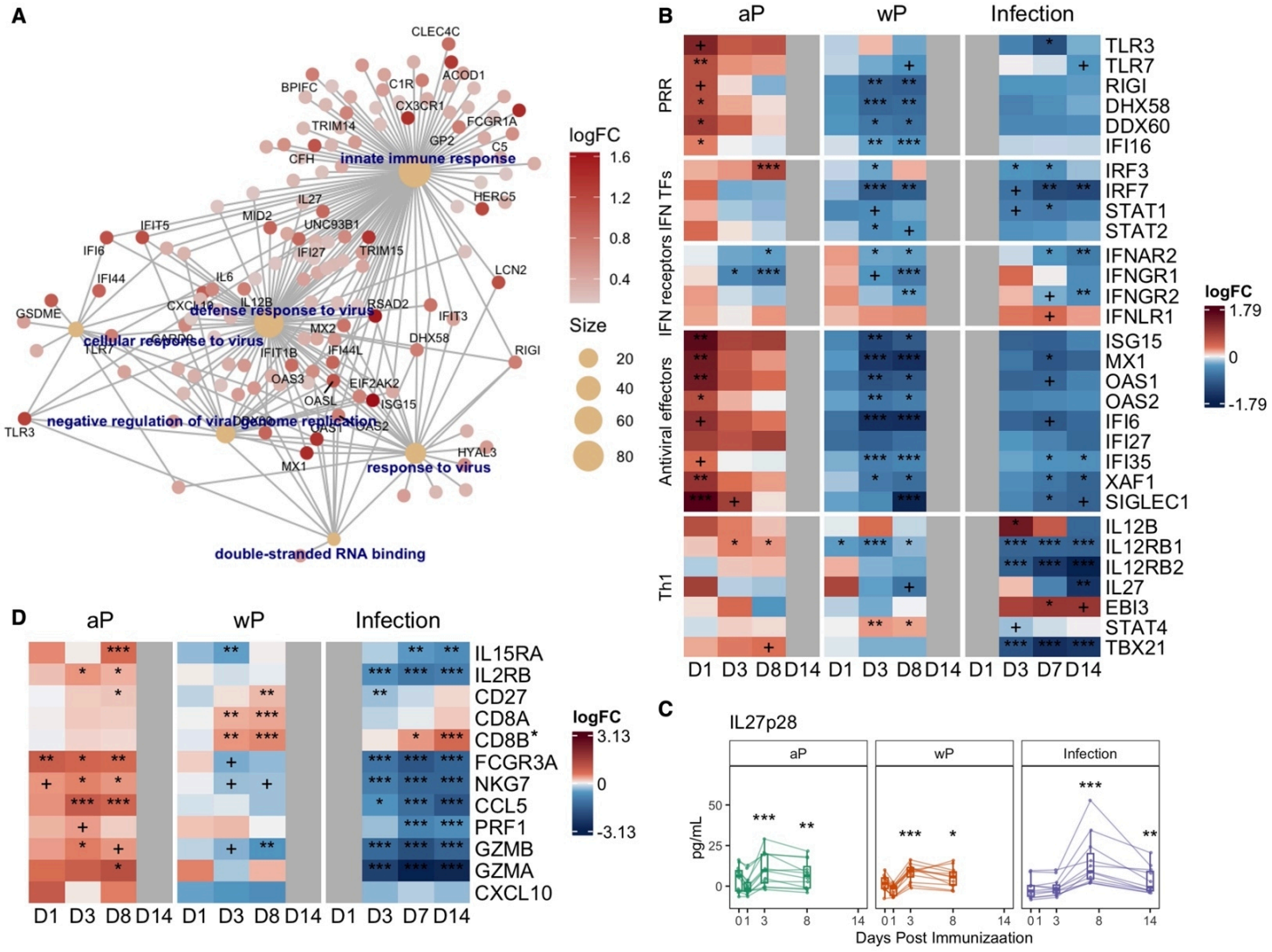


Figure 2

Strong antiviral responses observed in baboons received commercial multicomponent aP vaccinations but not wP vaccinations.

A)Network plot of antiviral gene set enrichment. Significantly enriched antiviral gene sets from GSEA analysis of day 1 post aP vaccination were plotted with nodes representing gene sets and individual genes, and edges indicating membership of a gene in a gene set. Node color of the gene indicates the logFC relative to baseline. Gene names are shown only for genes with more than 1.5-fold increase. **B)** Heatmap of antiviral related gene expression across group and time. **C)** Serum IL-27p28 production following vaccination or infection. Statistical comparisons were performed for each time point relative to their corresponding baseline (D0) within each group using paired Wilcoxon signed-rank test. **D)** Heatmap of cytotoxic effector related gene expression across group and time. The heatmaps show log2 fold changes (logFC) of selected genes grouped into functional programs. Columns represent time points days post immunization for each group. Color indicates logFC relative to their respective baseline. Differentially expressed genes between each time point and their baseline were shown. (*** P £0.001, ** P £0.01, * P £0.05, + P £0.1)

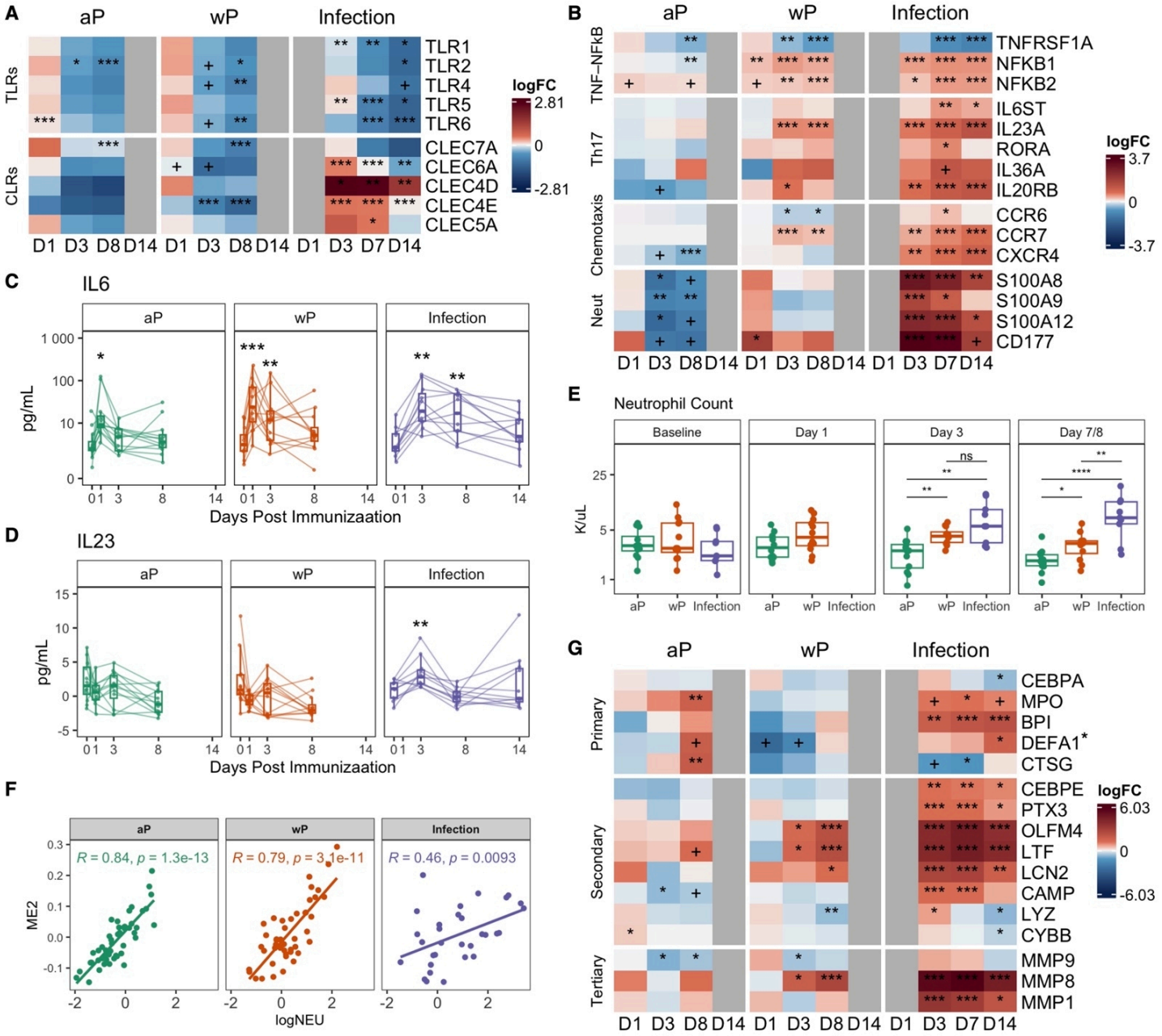


Figure 3

Pertussis infection and wP vaccination engage an NFkB–Th17–neutrophil inflammatory axis.

A)Heatmap of gene expression for pattern recognition receptors (PRRs) across groups and time points. **B)** Heatmap of genes associated with NFkb, Th17, and neutrophil signaling. Serum cytokine levels of **C)** IL-6, and **D)**IL-23 are shown over time. **E)** Neutrophil counts at early time points across groups. Data are presented as median with interquartile range. Statistical comparisons were performed between groups for each timepoints with Mann–Whitney U test. **F)** Correlation between WGCNA ME2 and log-transformed neutrophil counts for each group, with corresponding correlation coefficient (r) and p-value indicated. **G)** Heatmap of neutrophil granule associated gene expression. The heatmaps show log2 fold changes (logFC) of selected genes grouped into functional programs. Columns represent time points days post immunization for each group. Color indicates logFC relative to their respective baseline. Differentially expressed genes between each time point and their baseline were shown. (**** P £0.0001, *** P £0.001, ** P £0.01, * P £0.05, + P £0.1).

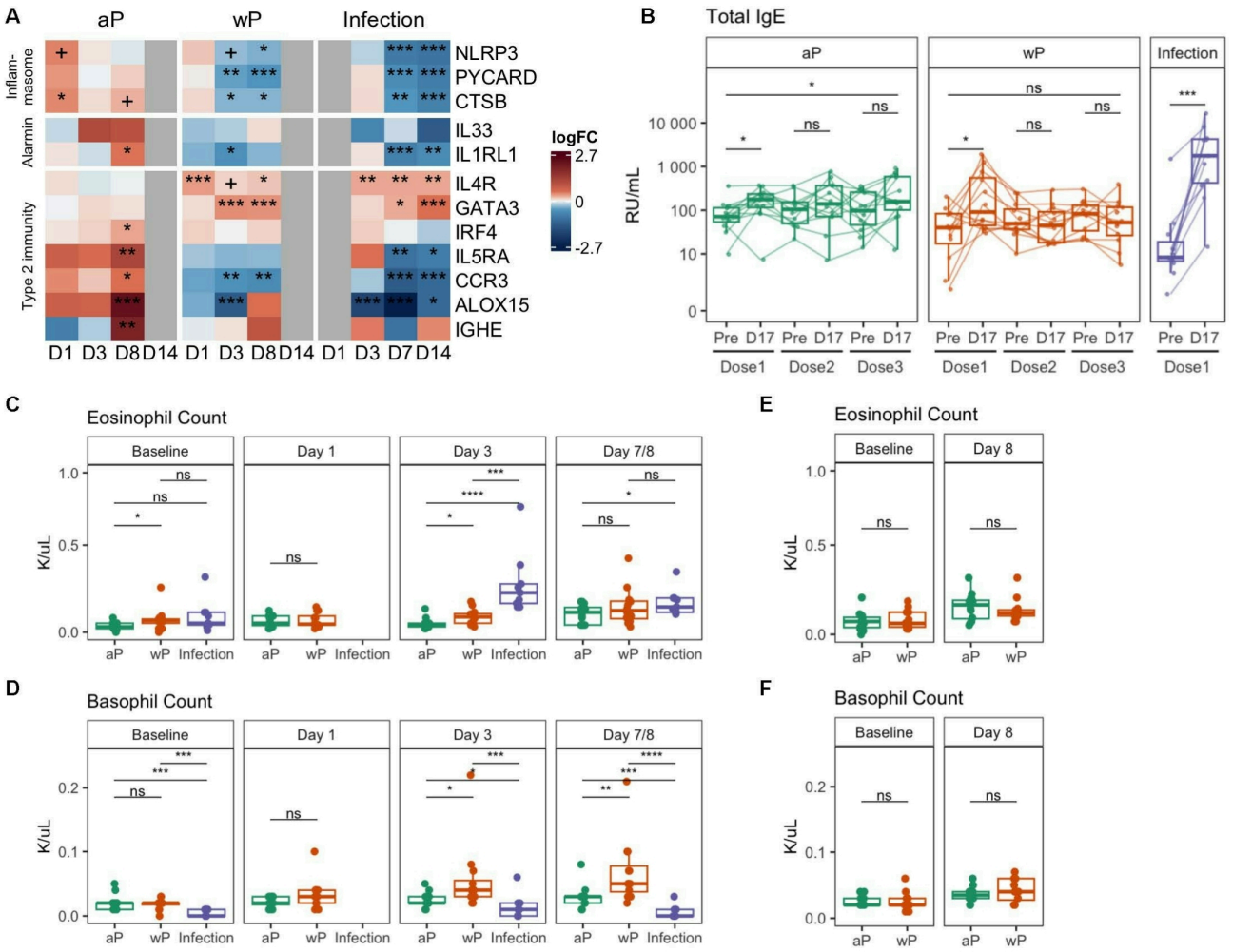


Figure 4

Th2 and related effector signatures.

A)Heatmap of genes associated with inflammasome activation, alamin, and type 2 immunity. The heatmap shows log2 fold changes (logFC) of selected genes grouped into functional programs. Columns represent time points days post immunization for each group. Color indicates logFC relative to their respective baseline. Differentially expressed genes between each time point and their baseline were shown. **B)** Total IgE levels in serum following vaccination or infection. **C)**Eosinophil and **D)** basophil counts following first dose of vaccination or infection. **E)** Eosinophil and **F)** basophil counts following second dose of vaccination. Data are presented as median with interquartile range. Statistical comparisons in **B)** to **F)** were performed between groups for each timepoints with Mann–Whitney U test. (**** P £0.0001, *** P £0.001, ** P £0.01, * P £0.05, + P £0.1)

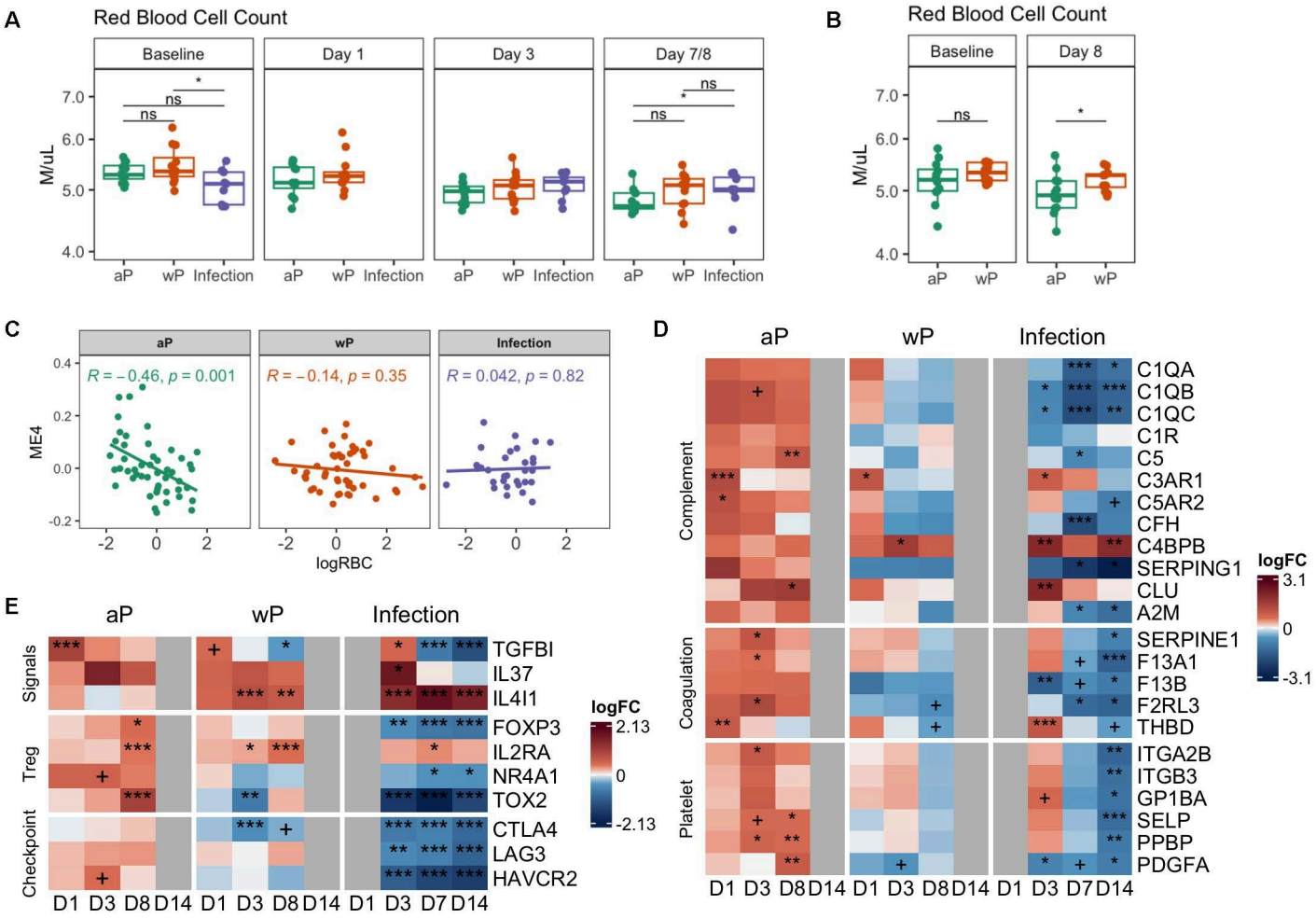


Figure 5

Cellular and transcriptional signatures related to erythropoiesis, immunothrombosis, and immune regulatory responses.

Red blood cell counts after **A)** first and **B)** second dose of vaccinations or infection. Data are presented as median with interquartile range. Statistical comparisons were performed between groups for each timepoints with Mann–Whitney U test. **C)** Correlation between WGCNA ME4 and log-transformed red blood cell counts for each group, with corresponding correlation coefficient (r) and p-value indicated. **D)** Heatmap of genes associated with complement activity, coagulation, and platelet activation. **E)**Heatmap of genes associated with immune regulatory signatures. The heatmaps show log2 fold changes (logFC) of selected genes grouped into functional programs. Columns represent time points days post immunization for each group. Color indicates logFC relative to their respective baseline. Differentially expressed genes between each time point and their baseline were shown. (**** P £0.0001, *** P £0.001, ** P £0.01, * P £0.05, + P £0.1)

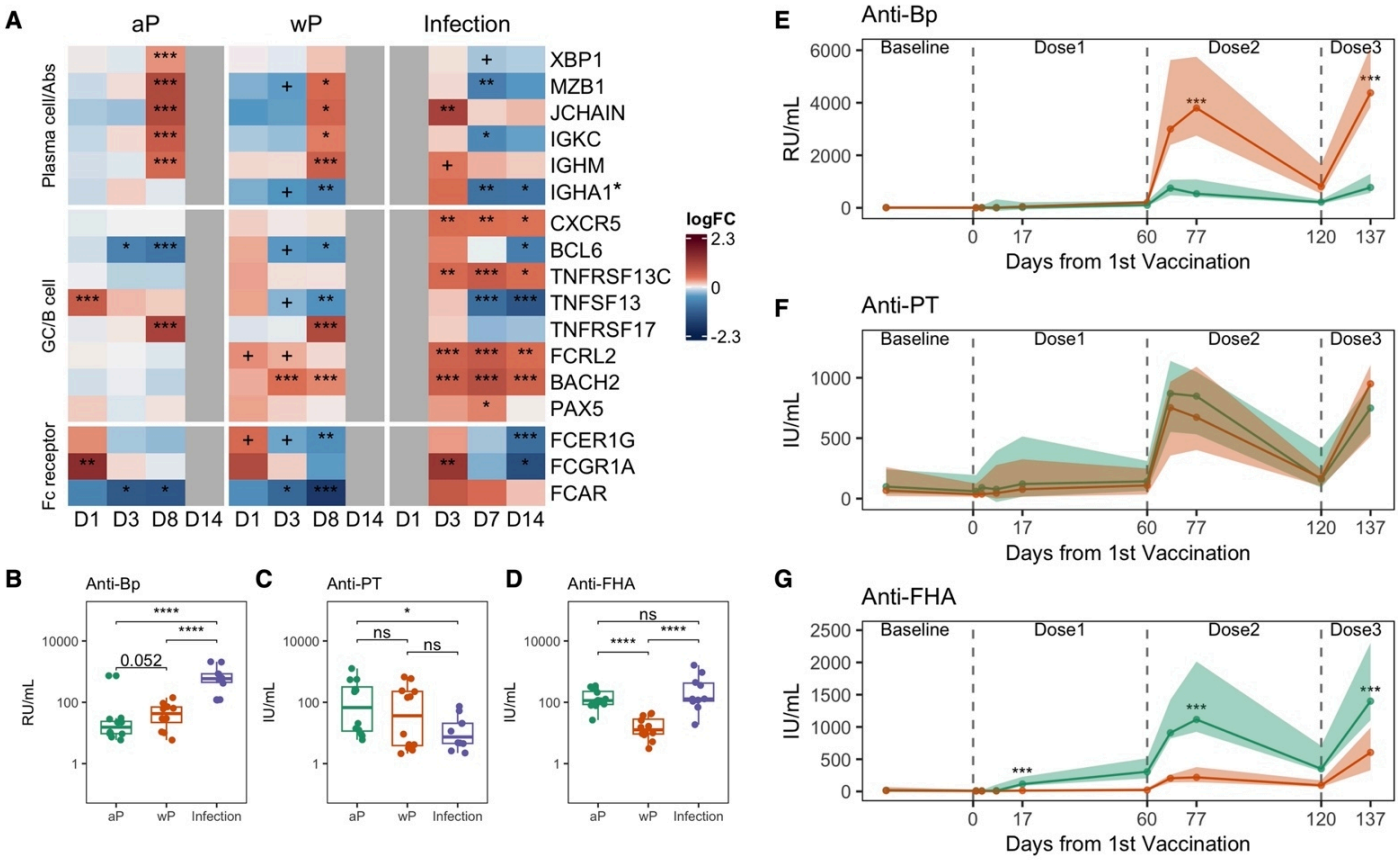


Figure 6

Differential signatures related to humoral immune responses and pertussis specific serum antibody levels across groups.

A)Heatmap of genes associated with plasma cell, germinal center, and memory B cell signatures. The heatmap shows log2 fold changes (logFC) of selected genes grouped into functional programs. Columns represent time points days post immunization for each group. Color indicates logFC relative to their respective baseline. Differentially expressed genes between each time point and their baseline were shown. Serum IgG titers on day 17 following the initial exposure against **B)** HKBp, **C)** PT, and **D)** FHA were evaluated. Data are presented as median with interquartile range. Serum IgG titers following each dose of aP and wP vaccinations against **E)** HKBp, **F)** PT, and **G)**FHA were evaluated. Lines represent group-wise medians, and shaded areas indicate the 95% confidence intervals. Statistical comparisons in **B)** to **G)**between groups were performed using Mann–Whitney U test. (**** P £0.0001, *** P £0.001, ** P £0.01, * P £0.05, + P £0.1)

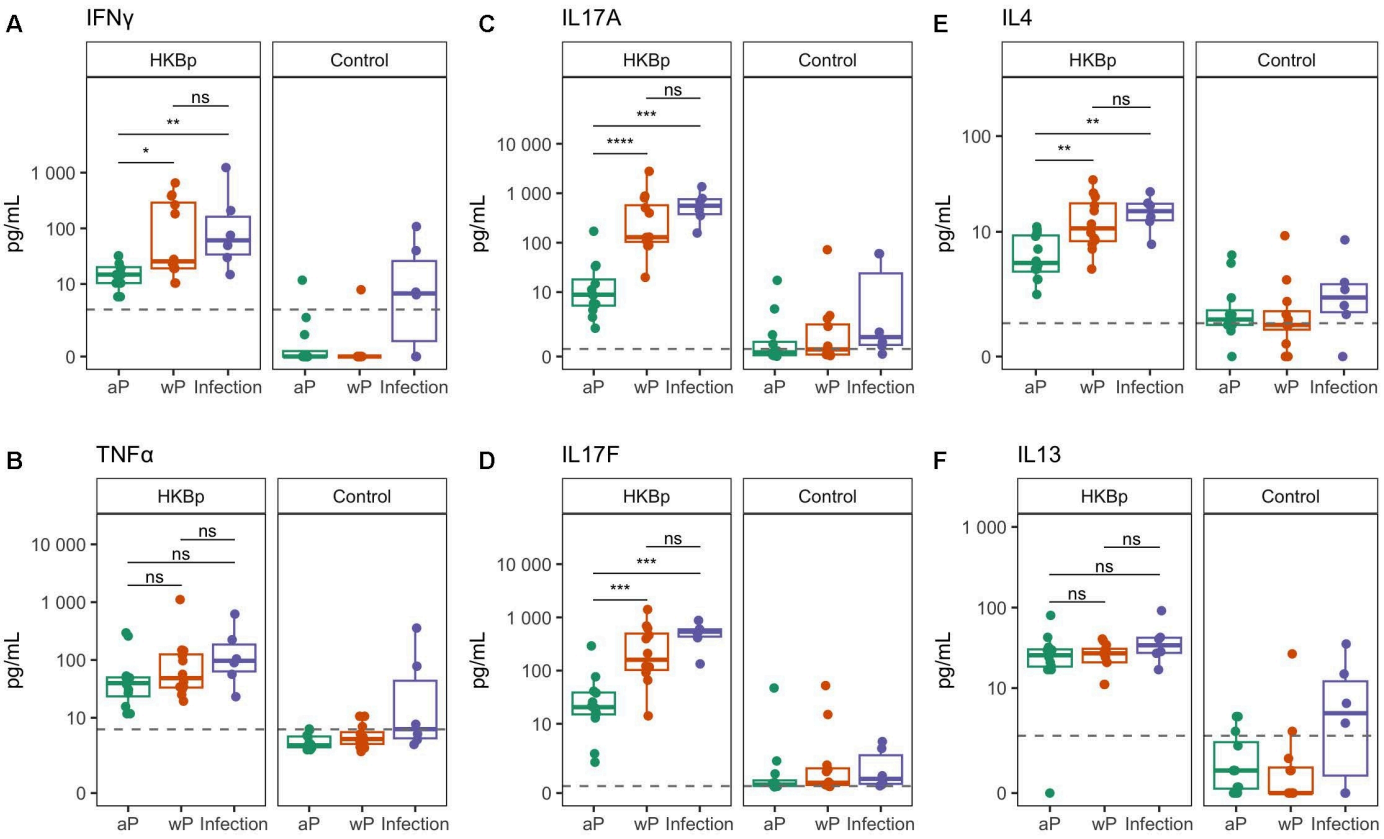


Figure 7

Cellular immune responses post vaccinations and pertussis challenge.

Cytokine productions of **A)** IFN-γ, **B)** TNF-α, **C)** IL-17A, **D)** IL-17F, **E)** IL-4, and **F)** IL-13 were evaluated in supernatant of PBMCs stimulated with HKBp compared to unstimulated control. PBMCs isolated on day 17 post the third dose of aP and wP vaccinations and on day 14 post pertussis infection were restimulated with HKBp for 72 hours before collecting for supernatant. Data are presented as median with interquartile range. Statistical comparisons between groups were performed using Mann–Whitney U test. (**** P £0.0001, *** P £0.001, ** P £0.01, * P £0.05)

Supplementary Files

This is a list of supplementary files associated with this preprint. Click to download.

- SupplementalTables.zip
- Table1and2.docx